

**MODELLING TRANSMISSION DYNAMICS OF  
TYPHOID FEVER WITH FEAR OF INFECTION AND  
VACCINATION IN KENYA**

**JACKLINE WANJIKU WANGUI**

**A PROJECT SUBMITTED IN PARTIAL FULFILLMENT  
OF THE REQUIREMENTS FOR THE AWARD OF THE  
DEGREE OF MASTER OF SCIENCE IN APPLIED  
MATHEMATICS OF THE UNIVERSITY OF EMBU**

**MARCH, 2025**

## DECLARATION

This project is my original work and has not been presented elsewhere for a degree or any other award.


Signature.......... Date..20/03/2025.....

Jackline Wanjiku Wangui

B527/1617/2022

Department of Mathematics and Statistics


This project has been submitted for examination with our approval as the University Supervisors.

Signature.......... Date.....21/03/2025.....

Dr. Marilyn Ronoh

Department of Mathematics and Statistics

University of Embu.

Signature.......... Date.....21<sup>st</sup> March 2025.....

Dr. Caroline Kanyiri

Department of Mathematics

Catholic University of East Africa

## **DEDICATION**

I dedicate this project to my loving parents, Francis and Ruth and to my beloved brother Joseph for their unwavering support, encouragement and understanding which fueled my determination and encouragement to overcome challenges. Their constant motivation and belief in my strengths and abilities inspired me to reach great heights. Their unwavering love and guidance instilled the courage to pursue my dreams relentlessly. Every milestone achieved is a testimony to my family's love and dedication. I also dedicate this work to my loving boyfriend, Shadrack, whose encouragement have been a guiding light to pursue my dreams.

## **ACKNOWLEDGMENT**

First, I am grateful to God for his favor, protection and blessings upon my life. It has taken His greatness to reach this far. I extend my deepest acknowledgments and gratitude to my esteemed supervisors; Dr. Marilyn Ronoh and Dr. Caroline Kanyiri, for their exceptional guidance, mentorship, motivation and expertise in this work. Their unwavering support, constructive feedback and encouragement have not only refined the quality of this work but have also nurtured my skills and growth as a researcher and a scholar. I also express my appreciation to Dr. Edna Manda, whose expertise have been instrumental in shaping the trajectory of this project. I am also immensely grateful to University of Embu for awarding me a scholarship and providing a conducive environment and organizing research workshops and opportunities that have facilitated the realization of this project. I am deeply indebted to my friends, Veronicah, Kawira, Hellen, Caroline, Bernard, Felix, Davey and Peter for your guidance, support and company in this academic journey. Finally, I express my gratitude to all persons who directly and indirectly contributed to the success of this project. Your collective support and contributions have been invaluable. May God bless you all abundantly.

## TABLE OF CONTENTS

<b>DECLARATION</b> .....	Error! Bookmark not defined.
<b>DEDICATION</b> .....	iii
<b>ACKNOWLEDGMENT</b> .....	iv
<b>LIST OF TABLES</b> .....	vii
<b>LIST OF FIGURES</b> .....	viii
<b>LIST OF ABBREVIATIONS AND ACRONYMS</b> .....	ix
<b>DEFINITIONS OF TERMS</b> .....	x
<b>LIST OF SYMBOLS</b> .....	xi
<b>ABSTRACT</b> .....	xii
<b>CHAPTER ONE</b> .....	1
<b>INTRODUCTION</b> .....	1
1.1 Background Information. ....	1
1.2 Statement of the Problem .....	2
1.3 Justification of the Study.....	3
1.4 Significance of the Study .....	3
1.5 Research Questions .....	4
1.6 Objectives of the Study .....	4
1.6.1 General Objective.....	4
1.6.2 Specific Objectives.....	4
1.7 Scope of the Study.....	4
<b>CHAPTER TWO</b> .....	5
<b>LITERATURE REVIEW</b> .....	5
2.1 Introduction .....	5
2.2 Modelling the Dynamics of Typhoid Fever .....	5
2.3 Research gap .....	9
<b>CHAPTER THREE</b> .....	11
<b>METHODOLOGY</b> .....	11
3.1 Introduction .....	11
3.2 Model formulation.....	11
3.3 Proposed model flow chart and equations.....	16
3.3.1The proposed model flow chart, Figure 1 .....	16
3.3.2 Model Equations .....	16
3.4 Model Analysis.....	16
3.4.1 Invariant Region.....	17

3.4.2 Positivity of Solutions .....	17
3.4.3 Boundedness of Solutions .....	17
3.4.4 Disease-Free Equilibrium.....	17
3.4.5 Basic Reproduction number ( $R_0$ ) .....	17
3.4.6 Local Stability of Disease-Free Equilibrium Point .....	18
3.4.7 Global Stability of Disease-Free Equilibrium Point .....	18
3.4.8 Endemic Equilibrium Point.....	18
3.4.9 Local Stability of EEP .....	18
3.4.10 Global Stability of EEP .....	18
3.5 Parameter Estimation .....	18
3.6 Numerical simulation .....	18
<b>CHAPTER 4 .....</b>	<b>19</b>
<b>RESULTS AND INTERPRETATIONS .....</b>	<b>19</b>
4.1 Positivity and Boundedness of Solutions .....	19
4.2 Invariant Region .....	19
4.3 Positivity of Solutions. ....	20
4.4 Boundedness of Solutions. ....	23
4.5 Disease-Free Equilibrium (DFE).....	25
4.6 The Basic Reproduction Number ( $R_0$ ) .....	25
4.7 Local Stability of Disease-Free Equilibrium (DFE) .....	28
4.8 Global Stability of the DFE.....	30
4.9 The Endemic Equilibrium Point.....	32
5.0 Global Stability of Endemic Equilibrium.....	33
6.0 Numerical Simulation .....	34
6.1 Parameter Estimation .....	35
6.1.1 Numerical Results .....	35
<b>CHAPTER FIVE.....</b>	<b>52</b>
<b>DISCUSSION, CONCLUSION AND RECOMMENDATIONS .....</b>	<b>52</b>
5.1 DISCUSSION AND CONCLUSION .....	52
5.2 RECOMMEDATIONS.....	54
<b>REFERENCES .....</b>	<b>55</b>

## LIST OF TABLES

<b>Table 1: Description of State Variables</b> .....	13
<b>Table 2: Description of Parameters</b> .....	14
<b>Table 3: Parameter Values</b> .....	36

## LIST OF FIGURES

<b>Figure 1:</b> Model Flow Chart.....	16
<b>Figure 2:</b> Numerical Solution of the Model. ....	37
<b>Figure 3:</b> Subplots of the Model.....	38
<b>Figure 4:</b> Effects of varying $\psi f$ on human populations when $\alpha$ is fixed at 0.1 and 0.9 respectively.....	39
<b>Figure 5:</b> Effects of varying $\psi f$ on recovered and bacteria populations when $\alpha$ is fixed at 0.1 and 0.9 respectively. ....	40
<b>Figure 6:</b> Effects of Varying $\eta_1$ and $\eta_2$ when $\alpha = 0.5$ and $\psi f = 0.5$ . ....	41
<b>Figure 7:</b> Effects of Varying $\eta_1$ and $\eta_2$ when $\alpha = 0.5$ and $\psi f = 0.5$ . ....	42
<b>Figure 8:</b> Effects of Varying $C_h$ on the susceptible population when $C_e$ is fixed at 0.1 and 0.9 respectively. ....	42
<b>Figure 9:</b> Effects of Varying $C_h$ when $C_e$ is fixed at 0.1 and 0.9 respectively. ....	43
<b>Figure 10:</b> Effects of Varying $C_h$ when $\psi f$ is fixed at 0.1 and 0.9 respectively. ....	44
<b>Figure 11:</b> Effects of Varying $C_h$ when $\psi f$ is fixed at 0.1 and 0.9 respectively. ....	45
<b>Figure 12:</b> Effects of Varying $C_h$ when $\alpha$ is fixed at 0.1 and 0.9 respectively. ....	46
<b>Figure 13:</b> Effects of Varying $C_h$ when $\alpha$ is fixed at 0.1 and 0.9 respectively. ....	47
<b>Figure 14:</b> Effects of Varying $C_e$ when $\psi f$ is fixed at 0.1 and 0.9 respectively. ....	48
<b>Figure 15:</b> Effects of Varying $C_e$ when $\psi f$ is fixed at 0.1 and 0.9 respectively. ....	49
<b>Figure 16:</b> Effects of Varying $C_e$ when $\alpha$ is fixed at 0.1 and 0.9 respectively. ....	49
<b>Figure 17:</b> Effects of Varying $C_e$ when $\alpha$ is fixed at 0.1 and 0.9 respectively. ....	50

## LIST OF ABBREVIATIONS AND ACRONYMS

<b>DFE</b>	Disease-free equilibrium
<b>GOK</b>	Government of Kenya
<b>MOH</b>	Ministry of Health
<b>MOE</b>	Ministry of Education
<b>ODE</b>	Ordinary Differential Equation
<b>PSIT</b>	Protected, Susceptible, Infected, and Treated Compartment.
<b>SDGs</b>	Sustainable Development Goals
<b>SEIR</b>	Susceptible, Unprotected, Infected, and Recovered
<b><i>S. typhi</i></b>	<i>Salmonella Typhi</i>
<b>TCV</b>	Typhoid Conjugate Vaccines
<b>WASH</b>	Water, Sanitation, Hygiene
<b>WHO</b>	World Health Organization

## **DEFINITIONS OF TERMS**

Typhoid fever	It is also known as enteric fever. The bacterial infection transmitted through contaminated food and water.
Infection	The process by which a bacteria multiplies in the human body after ingestion.
Transmission	The process by which an infection passes from one place or person to another.
Endemic	A situation where a particular disease is consistently present in a certain geographic area, such as a state or country.
Developing country	A country with low standards of living and average development.
Intervention	Act of modifying system's variables, parameters that leads to a change in the system's behavior or state influencing the system toward desired outcomes.
Perforation	An internal hole that develops through the walls of a body organ.
Risk factors	Attributes or exposures that necessitate and increase the likelihood of a person being infected by a disease.

## LIST OF SYMBOLS

$\mu$	mu
$\lambda$	lambda
$\varepsilon$	epsilon
$\omega$	omega
$\tau$	tau
$\eta$	eta
$\psi$	psi
$\beta$	beta
$\alpha$	alpha
$\delta$	delta
$\rho$	rho

## ABSTRACT

Despite the great advancements in healthcare systems and sanitary improvements globally, sub-Saharan Africa including Kenya bears a significant burden of infectious diseases, among which typhoid fever continues to exert a notable toll. In this study, we developed a deterministic mathematical model to examine the interplay between human responses driven by the psychological factor of fear of infection, vaccination efforts, and the dynamics of human-to-human and environmental transmission of typhoid fever. The mathematical model was analyzed using theories of first-order ordinary differential equations to establish the existence of equilibrium points and their conditions for local and global stability. The reproduction number,  $R_0$ , was established and distinct pathways for the transmission of infection were identified, shedding light on the crucial interactions among key population groups fueling the spread of typhoid fever disease. The model results suggest that, typhoid fever infection is heightened by both direct and indirect contact with infected individuals and contaminated environments. Additionally, lack or limited awareness contributes to decreased fear of infection and reluctance towards vaccination, further exacerbating the situation. Moreover, an increase in environmental transmission is observed due to elevated discharge rates from infected individuals. This study contributes valuable insights into the design of effective mitigation strategies aimed at combating typhoid fever in resource-limited settings.

# CHAPTER ONE

## INTRODUCTION

### 1.1 Background Information.

Typhoid fever continues to present a global hazard, resulting in over 21 million infections and 200,000 fatalities annually (Ayoola, 2021). The disease is particularly endemic in sub-Saharan Africa, with about 400,000 incidences annually and a high mortality rate of about 0.762% (Kim et al., 2022). The high rates of morbidity and mortality associated with this infection can be partially attributed to the emergence and the spread of drug-resistant *Salmonella Typhi* bacteria, fueled by the widespread use of second-generation antibiotics such as ciprofloxacin and levofloxacin, which diminishes the efficacy of these antibiotics against this pathogen (Mina et al., 2023). In sub-Saharan Africa, including Kenya, a significant proportion of the population resides below the poverty line, inhabiting densely populated areas characterized by poor sanitation and heightened exposure to infected individuals and contaminated environments (Ng et al., 2023). These crowded spaces often lack adequate sanitation facilities, leaving vulnerable demographics, such as infants and school-going children, particularly susceptible to adverse health effects from typhoid fever infection and other infectious diseases (Antillón et al., 2017).

Typhoid fever is endemic in Kenya, with approximately 126,000 incidences reported every year and frequent outbreaks observed in central, coastal and western parts of Kenya (Adi, 2018). Most of these outbreaks were traced to limited access to clean water sources, inadequate latrines, and poor hygiene facilities, particularly among street food vendors and their clients (Adi, 2018). Notably, in early 2023, Kenya reported an outbreak at one local secondary school in Western Kenya involving 1062 patient cases, predominantly students, which resulted in a number of mortality cases (WHO, 2023). The outbreak was attributed to contaminated food, poor personal hygiene and untreated water (WHO, 2023). In most developing countries, prevention and control of typhoid fever disease include drinking treated water, proper sanitation, vaccination and adequate medical care (Mushanyu et al., 2018).

Recent advancements in vaccination have contributed greatly to reduced incidences of typhoid fever globally (Kim et al., 2022). However, widespread rollout of typhoid fever vaccine as a routine tool for disease prevention in many endemic regions in sub-

Saharan Africa continues to face significant hurdles (Duncan et al., 2020). Lack of adequate knowledge about typhoid fever vaccine, declining efficacy of typhoid fever vaccines over time, insufficient funding to support widespread vaccine rollout due to government priorities, inadequate health infrastructure, cultural and religious beliefs, community norms, vaccine hesitancy fueled by misinformation and distrust in healthcare systems are some of the factors hindering the uptake and efficacy of typhoid fever vaccines in endemic regions (Meiring et al., 2019). In addition, accessibility and affordability present significant challenges in sub-Saharan Africa, with vaccines potentially inaccessible due to cost or logistical hurdles (Addy, 2024). Implementing effective and affordable strategies is urgently required in most affected and high-risk populated areas to effectively control typhoid fever in resource-limited regions (Stanaway et al., 2020).

To further aid the understanding of typhoid fever dynamics, novel tools such as mathematical models have been employed to provide key insights influencing the spread of this disease and forecast potential interventions for effectively mitigating the disease (Edward, 2017, Matsebula, 2021, Mushayabasa, 2016, Volkova et al., 2013). Very few of these studies considered a combination of psychological factor of fear of infection and vaccination as control strategies. Historically, human behavior has been intricately linked to the dynamics of infectious diseases and therefore their understanding is key for effective control and management of infectious diseases such as typhoid fever (Verelst et al., 2016). Hence, the objective of this research study is to examine the effects of the psychological factor of fear of infection combined with vaccination in the transmission dynamics of typhoid fever while factoring in the direct and indirect modes of transmission. This study seeks to contribute valuable insights into the design of effective mitigation strategies aimed at combating typhoid fever in resource-limited settings.

## **1.2 Statement of the Problem**

Despite global efforts in health care and sanitation to combat typhoid fever, it remains tenacious and alarming in areas where safe drinking water and proper sanitation are compromised. The infection greatly burdens the public and local health, leading to high morbidity and mortality rates. In addition, its impact on the socio-economic status hinders development and perpetuates poverty.

Several Mathematical models have been formulated for enhanced understanding in the transmission dynamics of typhoid disease. Most of these models have incorporated various factors for example; seasonality (Matsebula, 2021), limited public health resources (Mushanyu et al., 2018), drug resistance (Kanyi et al., 2021), antibiotic resistance (Volkova et al., 2013), and optimal screening (Mushayabasa, 2016) among others. However, very few models have taken into consideration the psychological factor of fear as an indispensable component in the human response to typhoid fever disease as well as vaccination which may subject to low achievement of the SDGs. Therefore, this study will incorporate the role of fear and vaccination in both direct and indirect transmission modes which has not been investigated before. Thus, this work will give a deeper understanding of how the aspect of fear influences people's actions and perceptions during outbreaks of typhoid fever disease as well as how they respond to vaccination.

### **1.3 Justification of the Study**

Despite numerous studies being done by several researchers on the modeling of typhoid fever, there is few investigations on the modeling of typhoid fever considering the impact of human response to a disease. The disease is prevalent in densely populated areas and in low-income countries where poor hygiene, food, and water contamination are common. Since typhoid fever is an infectious disease, its outbreak causes severe complications which can be fatal and affect the socioeconomic status of the population affected.

Understanding the basic mechanism of disease transmission is important for effective prevention and control strategies against typhoid fever. Mathematical modeling provides a unique approach to key insights into the dynamics of infectious diseases like typhoid fever. Thus, the study explores the impact of fear and vaccination as a disease control strategy, which reduces typhoid infection towards achieving sustainable development goals (SDGs).

### **1.4 Significance of the Study**

The study model formulated helps public medical officers understand the transmission dynamics of typhoid fever and aid in decision-making on infectious disease intervention programs. In addition, this research work will broaden the potential of

researchers and scientists in the field of modeling the importance of human behavioral aspects in the spread of diseases.

### **1.5 Research Questions**

1. How do human behavior and vaccination affect the transmission of typhoid fever?
2. How is the deterministic model well-posed in presence of fear of infection and vaccination in typhoid dynamics?
3. What is the impact of human behavior and vaccination on the spread of typhoid fever disease?

### **1.6 Objectives of the Study**

#### **1.6.1 General Objective**

To formulate a deterministic mathematical model that incorporates human behavior (fear) and vaccination in the control of typhoid fever transmission from both human to human and environment to human.

#### **1.6.2 Specific Objectives**

1. To formulate a deterministic mathematical model incorporating fear as a human behavioral aspect and vaccination in the spread of typhoid.
2. To analyze the model based on reproduction number and theories of first-order ordinary differential equations.
3. To perform numerical simulations to investigate the impact of fear and vaccination on typhoid fever transmission.

### **1.7 Scope of the Study**

Other risk factors contribute to the causes of typhoid fever disease but this study considers *S. typhi* bacteria as the primary cause of typhoid fever disease (Kaluse *et al.*, 2021). *S. typhi* bacteria is spread by contaminated food, and untreated water and is most prevalent in highly populated areas. Thus, this study is limited to *S. typhi* bacteria as the main cause of typhoid fever to model typhoid fever dynamics incorporating psychological factor of fear in both modes of transmission of typhoid fever.

## CHAPTER TWO

### LITERATURE REVIEW

#### 2.1 Introduction

Mathematical modeling of infectious diseases is vital in studying the disease trend and making an analysis on how they can be mitigated. Several researchers have improved the SIR model for typhoid fever disease thus providing reasonable results.

#### 2.2 Modelling the Dynamics of Typhoid Fever

The study done by Edward, (2017) aimed to model the transmission dynamics through the direct and indirect routes. Mathematical features such as the threshold for the epidemic, steady states, positivity, and boundedness were well determined. The results showed that elevated discharge rates of the bacteria concentration to the environment by either symptomatic or asymptomatic individuals increased the potential to contract the bacteria from the contaminated environment. Also, heightened direct contact with individuals who are either the symptomatic or asymptomatic increased the vulnerability to contract the infection. It was concluded that minimizing contact with the typhoid carriers, avoiding contaminating water sources with feces, and using latrines can minimize the transmission rate. The model had shortcomings since the approach did not account for public education initiatives, which is a key aspect in creating societal awareness about the transmission and prevention against typhoid fever disease. Therefore, the researcher suggested that education can be utilized as a preventive approach against typhoid fever and that it can lessen the disease transmission when combined with other control techniques like vaccination, improved sanitation, and consideration of biological concentration with bacteria. To fill this gap, we have incorporated the aspect of vaccination and taken into consideration the role of fear which drives people to improve their hygiene and sanitation. The fear aspect is modeled as a parameter that is between 0 and 1. When the parameter is 0 it means people lack awareness of the disease and the only way we can create this awareness is through educational campaigns.

Edward & Nyerere, (2017) developed a deterministic mathematical model to assess the impact of education campaigns, vaccination, and treatment on controlling the dynamics of typhoid fever. The model divided their population into five subgroups

namely; susceptible  $S(t)$ , vaccinated  $V(t)$ , infectious  $I(t)$ , typhoid carriers  $I_c(t)$ , and the recovered individuals  $R(t)$ . Thus, the formulated mathematical model was;  $N = S + V + I + I_c + R$ . The result indicated that controlling typhoid fever depends on different factors and sectors like education sectors, sanitation sectors, and water supply organizations as well as the health care sectors. Thus, it was recommended that any typhoid control program must pool resources with population-level education of susceptible and infected humans. The researchers concluded that various control strategies working collaboratively are more effective than a single strategy. The model had two limitations which include; infection is transmitted through the direct mode only and that vaccination is a continuous state. Thus, it was proposed that the study can be modeled by impulsive differential equations since vaccination can be discontinuous and seasonal. To address this shortfall, our research model considers vaccination as a parameter that lie between 0 and 1 thus this range will take into consideration the seasonality, continuity and discontinuity of the vaccine.

Mutua et al., (2017) presented a compartmental model with an aim to investigate the influence of socioeconomic status and vaccination initiatives on transmission dynamics of typhoid fever. The model divided the susceptible individuals into two classes; susceptible high ( $S_h$ ) and susceptible low ( $S_l$ ). The two classes lead to infection ( $I$ )- person to person and infection ( $B$ ) environment to person. The infected recover at a certain rate ( $R$ ) or become asymptomatic ( $C$ ). The formulated model was presented as;  $N = S_h + S_l + I + B + R + C$ . Their findings portrayed that low socioeconomic status increases the rates of typhoid fever and the reproduction number. Further, increasing the vaccination in the low socioeconomic population results in a lower reproduction number thus lowering the prevalence of the disease. It was concluded that both low and high socioeconomic classes need to be considered by the vaccination programs for successful mitigation of typhoid fever disease. Our study assumes that everyone in the community is susceptible and get vaccinated at a rate  $\alpha$  thus taking into account all the classes.

Mushanyu et al., (2018) formulated a mathematical model using a nonlinear ordinary differential equation with a goal to assess the prospective outcome of scarce public healthcare resources on the prevention and control of typhoid fever. The model had five compartments namely, susceptible individuals ( $S$ ), infected individuals ( $I$ ),

carrier humans ( $C$ ), individuals under treatment ( $T$ ), and the recovered individuals ( $R$ ). The presented model was;  $N = S + I + C + T + R$ . The findings of the study showed that limited healthcare services or when impoverished individuals have inadequate access to treatment due to financial constraints increases the incidence of typhoid fever. The researchers concluded, that when treatment demand is minimal, then public health resources will be adequate for the treatment of typhoid patients thus minimizing transmission dynamics of typhoid fever in a particular community. It was recommended that communities should possess adequate resources for treating typhoid fever patients to reduce the spread of typhoid fever disease. Since there is limited medical facilities and only few benefits from them, our research bridges this scenario by incorporating vaccination against typhoid fever, which will aid in curbing the disease spread. Typhoid fever will thus be suppressed since the few people who contract it will be able to access the existing medical resources.

Gauld et al., (2018) developed an individual-based mathematical model of typhoid transmission including short cycle and long cycle transmission routes. The short cycle represents transmission of infections from humans to humans through food contamination agents. The model accurately reflected the endemicity, immunization, and environmental management dynamics in Santiago. The study model divided the human population into six compartments; unexposed, susceptible, incubating, acute infection, subclinical infection, and chronic carrier. The results showed that administration of typhoid fever vaccines can minimize the transmission, but they also emphasized the significance of locating and addressing the major long-cycle transmission channels to enable focused and long-lasting control. Additionally, typhoid incidence is expected to decrease as a result of the vaccine, according to estimates. Since the study recommended focusing on the long cycle and vaccination, our study incorporates the bacteria population in the model and vaccination in the model.

Karunditu et al., 2019) developed a deterministic *SEIR* mathematical model of typhoid fever incorporating unprotected humans in the spread of typhoid. This study aimed to examine the equilibrium points that is, both local and global stability. The model compartments were; Susceptible ( $S$ ), Unprotected ( $E$ ), Infective ( $I$ ), and Recovered ( $R$ ). Thus, the model formulated was;  $N = S + E + I + R$ . The model included

various parameters such as natural and induced mortality rates. The findings of the study suggested that the equilibrium points are stable when the reproduction number is less than one otherwise unstable. Therefore, if typhoid is to be mitigated effectively, then unprotected humans have to be considered with other protective factors since they greatly impact the spread of typhoid infection. It was concluded that there is a direct variable link between the two since a 10% increase in the unprotected raises the infectious. It was therefore advised that policymakers in the health sectors should include preventive measures to prevent the disease from prevailing in a given population, as unprotected humans play a crucial role in the spread of typhoid. In light of this, our research examines human influence and vaccination as preventative methods against typhoid fever to lessen typhoid fever.

Nyaberi & Musaili, (2021) formulated a model for the transmission dynamics of typhoid fever analyzing the impact of treatment of the infected on typhoid dynamics. The human population was divided into three compartments namely; susceptible ( $S$ ), infected ( $I$ ), and recovered ( $R$ ). Therefore, the  $SEIR$  model was;  $N = S + E + I + R$ . The results illustrated that the absence of treatment or ineffective treatment increases the infection rate and with effective treatment the number of infected individuals reduces. The researchers concluded that efficient treatment is beneficial in eradicating typhoid fever. The study assumed that typhoid fever is transmitted through direct modes only and neglected the fact that typhoid fever can be transmitted through indirect mode. Thus, to address this, our study considers both direct and indirect modes of typhoid fever transmission while incorporating a combination of control strategies, that is, human influence and vaccination to curb the transmission dynamics of typhoid fever disease.

Matsebula, (2021) did a mathematical analysis of typhoid fever transmission incorporating seasonality and fear. The model ( $N = S + I + R + B$ ) involved nonlinear differential equations with a time-dependent infection rate. The total human population was categorized into three sections as follows; susceptible ( $S$ ), infected ( $I$ ), recovered ( $R$ ), and the bacteria concentration in the environment ( $B$ ). The findings depicted that, poor hygiene, and unimproved wastewater management system, rainfall patterns especially in summer contributed heavily to the transmission dynamics. Additionally, the study concentrated more on the impact of seasonality on the basic

reproduction number, the count of steady states and their stabilities as well as their stability analysis. The researcher recommended that, investigating the role of human behavior, specifically fear with other control strategies, can help in mitigating typhoid fever, since individuals have a substantial impact on transmission of typhoid fever and bacterial infections. Thus, our study incorporates fear and vaccination as a control strategy in controlling typhoid fever disease.

Ryan, (2021) formulated a mathematical model to investigate the impact of hospitalization in the management of typhoid fever. The study aimed to determine the interrelationship between hospitalization rates and the contagiousness of typhoid fever over time. The human population was divided into six compartments that are, susceptible ( $S$ ), infectious ( $I$ ), carriers ( $C$ ), home-based care ( $H_b$ ), hospitalized ( $H$ ), and the Recovered ( $R$ ). The formulated model was presented as;  $N = S + I + \dots R$ . The findings showed that when  $R_0$  was less than unity an individual caused fewer than one occurrence of secondary infection thus the disease dies out otherwise it evades the given population. Additionally, healthcare management of typhoid patients contributes greatly to the mitigation of typhoid fever infections. When hospitalization is low the infection rate is high implying that increasing healthcare services reduces the infection rate thus mitigating typhoid fever. However, the study assumed the transmission modes of typhoid fever disease but recommended that greater attention should be given to the escalating number of typhoid fever carriers in the susceptible population. To address this, our study considers vaccination as a way of lessening the count of carriers in a given population and also considers direct and indirect modes of transmission of typhoid fever disease.

### **2.3 Research gap**

Studies on typhoid fever disease have been done using compartmental models involving stochastic differential equations Volkova *et al.*, (2013) and ordinary differential equations Kailan Suhuyini & Seidu, (2023). The study was done Matsebula, (2021) on modeling the transmission dynamics of typhoid fever with seasonality and fear stated that the model was theoretical and that in the presence of available data, the research would depict effective results. The study showed that investigating the role of human behavior such as fear remains a great interest in

bacterial infection. Since vaccination is the most common control technique in the event of a disease epidemic, this study work will include the fear parameter in the suggested model as well as the vaccination parameter as a control approach against infection.

Several models have been formulated to model the impact of various aspects like vaccination, treatment, migration, sanitation effects, and drug effects among others and they have assumed that direct contact is the only transmission route of transmission. Although several models have incorporated both direct and indirect modes of transmission for example, (James *et al.*, 2021) and (Edward, 2017), very few have incorporated the aspect of human behavior and vaccination in both direct and indirect modes of transmission. Therefore, there is an evidenced need for research-based information which can be vital to medical specialists and researchers. Thus, this study aims to fill the gap by developing a deterministic mathematical model to investigate the impact of psychological factor of fear and vaccination on typhoid fever dynamics.

## CHAPTER THREE

### METHODOLOGY

#### 3.1 Introduction

This chapter entails the methodology used in this research to achieve the objective stated in section 1.5.2. It entails model description and formulation, theories of the ordinary differential equations, and steps used in numerical simulation.

#### 3.2 Model formulation

We develop a mathematical model to examine the interplay between human responses driven by the psychological factor of fear of infection and vaccination efforts in the transmission dynamics of typhoid fever. This formulation takes into account both direct and indirect modes of typhoid fever transmission. The direct mode of typhoid fever transmission occurs through human-to-human contact via the fecal-oral route whereas the indirect transmission takes place when a susceptible individual ingests contaminated water or food that has been contaminated with *Salmonella typhi* bacteria typically sewage-contaminated water or food handled by an infected person Adi, (2018).

We categorize the human population into four classes such that at time  $t \geq 0$  there are susceptible individuals ( $S(t)$ ), infected individuals stemming from direct transmission resulting from human - human interaction ( $I_h$ ), infected humans stemming from indirect transmission resulting from human interaction with the contaminated environment ( $I_e$ ) and the recovered individuals ( $R$ ) following treatment. We also include the class  $B$ , which represents the bacteria population in the environment. The total size of the human population is given as  $N_h(t) = S(t) + I_h(t) + I_e(t) + R(t)$  and the total size of both the human and bacteria populations denoted by  $N(t)$  is given as  $N(t) = S(t) + I_h(t) + I_e(t) + R(t) + B(t)$ .

The susceptible class ( $S$ ) is free from typhoid fever infection but when in contact with infectious individuals ( $I_h, I_e$ ) or contaminated environments, they are at risk of typhoid fever infection at the incidences rates  $\beta_h, \beta_e$ , resulting from the direct and indirect

modes of transmission, respectively. The expressions for  $\beta_h$ , and  $\beta_e$  are given as follows:

$$\beta_h = \frac{(1-\psi_f)C_h(\eta_1 I_h + \eta_2 I_e)}{N_h}, \quad \beta_e = \frac{C_e(1-\psi_f)B}{K+B}$$
 where  $C_h$ , and  $C_e$ , denotes effective contact rate for typhoid fever transmission to occur for direct and indirect transmission, respectively. The parameters  $\eta_1$  and  $\eta_2$  represent the veracity of infection from infected individuals with *Salmonella typhi* bacteria, with  $\eta_1 < \eta_2$ , given that the probability of typhoid fever transmission for a susceptible individual in contact with an infected individual is lower compared to when a susceptible individual is in contact with a contaminated environment (Matsebula, 2021). Thus,  $\eta_1$ ,  $\eta_2$  are dimensionless parameters to differentiate the severity of the typhoid fever infection.

Parameter  $\psi_f$  represents the psychological factor of fear of infection which drives individuals to improve their sanitation, personal hygiene, and exercise care during meal preparations or purchasing food. We let  $0 < \psi_f < 1$  where  $\psi_f = 0$  implies that there is no dread to typhoid fever disease either due to lack of awareness or simply negligence and this significantly increases the contact rate which in turn fuels the spread of typhoid fever.  $\psi_f = 1$  implies that individuals are fully aware of the typhoid disease spread and its controls due to effective education campaigns. In this case, individuals are fully adherent to preventive measures and are fully aware of the consequences of neglecting sanitation and personal hygiene. Thus, fear of contracting the typhoid fever disease drives them to significantly limit any contact rate with possible sources of contamination and this reduces the spread of typhoid fever disease significantly. The behavioral dynamics can be linked to more immediate reactions in an emerging epidemic. The impact on disease dynamics might be extremely substantial if protective behavioral changes brought about by fear of contracting the disease is significantly high in the community. When people are self-aware of the disease and maintain proper sanitation, the disease is significantly reduced. However, numerous waves of infection may result from their later re-entry into the population when their dread fades.

The parameter  $K$  represents the carrying capacity of *Salmonella Typhi* bacteria in the environment such as water or food due to limited resources to sustain its growth

indefinitely.  $\frac{B}{B+K}$  represents the fraction of the carrying capacity  $K$  that is currently occupied by the bacteria population  $B$  in the environment. In this formulation, recruitment rate into the *Salmonella Typhi* bacteria population is described by a logistic growth equation  $b$ , given as  $b = rB (1 - \frac{B}{K})$  where  $r$  represents per capita growth rate of the bacteria population. The bacteria population is cleared from the environment at a rate  $\tau$ .

Parameter  $\alpha$  represents the proportion of the susceptible individuals who are vaccinated against typhoid fever disease. This study assumes that vaccination is a continuous process. Given that typhoid fever vaccination does not confer 100% protection against typhoid fever infection, the vaccinated population can become susceptible when the vaccination loses its efficacy, thus  $0 < \alpha < 1$ .  $\alpha = 1$  represents an ideal scenario where a highly efficacious typhoid fever vaccine guarantees permanent immunity against typhoid fever disease, whereas when  $\alpha = 0$ , implies that the susceptible population is not vaccinated.

Susceptible class ( $S$ ) is increased by natural birth  $\lambda$  and the recovered population that lose immunity at a rate  $\omega$  from the recovered class and is reduced by the newly infected individuals that move to the infected classes  $I_h$  and  $I_e$  as a result of the incidence rates  $\rho(1-\alpha)\beta_h$  and  $(1 - \rho)(1 - \alpha) \beta_e$  respectively. Parameter  $\rho$  represents the proportion of newly infected individuals as a result of contact with humans-to-humans interaction (direct mode) whereas  $1 - \rho$  represents newly infected individuals as a result of humans to environment interaction (indirect mode). Infected classes  $I_h$  and  $I_e$  are increased by the incidence rates  $\rho(1-\alpha)\beta_h$  and  $(1 - \rho)(1 - \alpha) \beta_e$  and all are decreased by the death due to infection  $\delta$  and recovery rate  $\varepsilon$ . The Recovered class ( $R$ ) increases due to the newly recovered individuals at a rate  $\varepsilon$ , and decreases due to individuals losing their immunity at a rate  $\omega$ , who then return to the susceptible class. Populations,  $S, I_h, I_e, R$  are further reduced to natural deaths at a natural death rate  $\mu$ .

**Table 1** and **Table 2** describe the variables and the parameters respectively. **Figure 1** describes the model flow chart. The resulting model equations are given in section 3.4.2.

**Table 1: Description of State Variables**

---

<b>Variables</b>	<b>Description</b>
$S(t)$	Susceptible human population at time $t$
$I_h(t)$	Infected humans resulting from direct transmission at time $t$
$I_e(t)$	Infected humans resulting from indirect transmission at time $t$
$R(t)$	Recovered human population at the time $t$
$B(t)$	Bacteria concentration in the environment at time $t$
$N_h(t)$	Total human population ( $S + I_h + I_e + R$ )

**Table 2: Description of Parameters**

---

<b>Parameter</b>	<b>Description</b>
$\lambda$	Recruitment rates into the susceptible populations through natural births
$\mu$	Natural death rate of individuals
$\psi_f$	Psychological factor of fear of typhoid fever infection
$\omega$	Rate at which the recovered individuals lose immunity
$\varepsilon_1$	Rate of newly recovered individuals from $I_h$
$\varepsilon_2$	Rate of newly recovered individuals from $I_e$

$\eta_1$	Dimensionless parameter representing veracity of typhoid fever infection when contact is between susceptible and $I_h$
$\eta_2$	Dimensionless parameter representing veracity of typhoid fever infection when contact is between susceptible and $I_e$
$\alpha$	Proportion of vaccinated susceptible Individuals
$\delta_1$	Disease induced death rates stemming from $I_h$
$\delta_2$	Disease induced death rates stemming from $I_e$
$\rho$	Proportion of newly infected individuals due to direct transmission mode
$\tau$	Clearance rate of the bacteria in the environment
$r$	Per capita growth rate of the bacteria population in the environment
$K$	Carrying capacity for the bacteria
$C_h$	Effective contact rate with infected humans
$C_e$	Effective contact rate with the contaminated environment

### 3.3 Proposed model flow chart and equations

#### 3.3.1 The proposed model flow chart, Figure 1

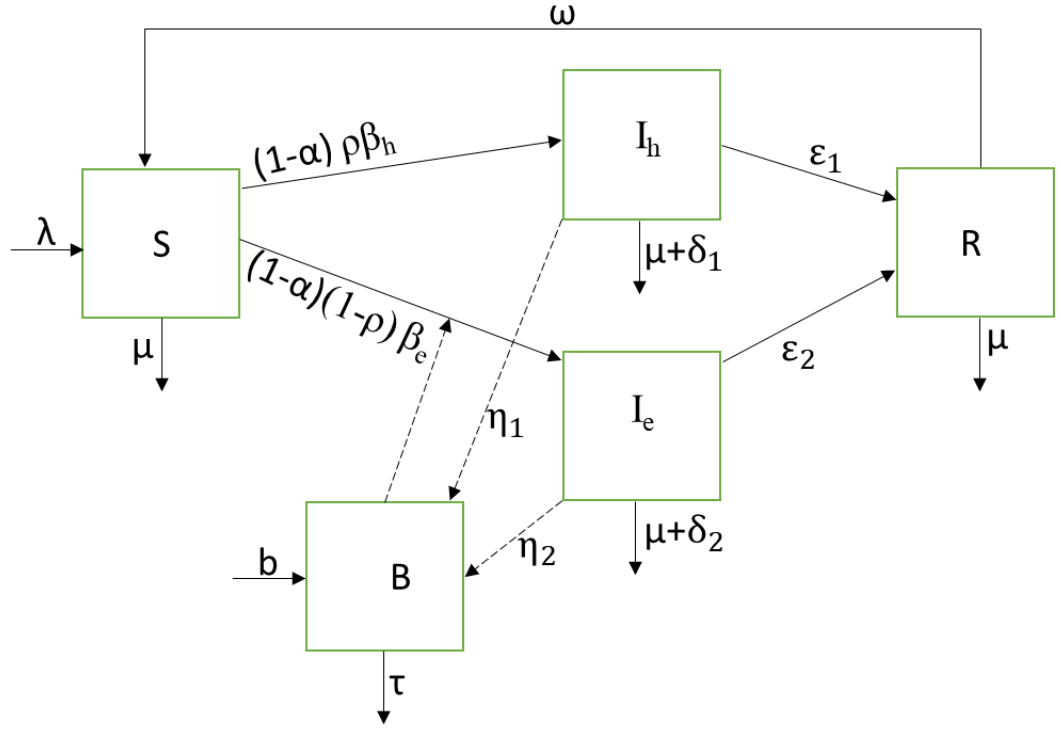


**Figure 1:** Model Flow Chart

#### 3.3.2 Model Equations

$$\frac{dS}{dt} = \lambda - (\rho\beta_h + (1 - \rho)\beta_e(1 - \alpha) - \mu)S + \omega R. \quad (1)$$

$$\frac{dI_h}{dt} = \rho\beta_h(1 - \alpha)S - (\mu + \delta_1 + \epsilon_1)I_h. \quad (2)$$

$$\frac{dI_e}{dt} = (1 - \alpha)(1 - \rho)\beta_e S - (\mu + \delta_2 + \epsilon_2)I_e. \quad (3)$$

$$\frac{dR}{dt} = \epsilon_1 I_h + \epsilon_2 I_e - (\mu + \omega)R. \quad (4)$$

$$\frac{dB}{dt} = b + (\eta_1 I_h + \eta_2 I_e) - \tau B. \quad (5)$$

#### 3.4 Model Analysis

This was done by proving several mathematical theorems, invariant region, positivity, equilibria, basic reproduction number, and the stabilities of the model.

### 3.4.1 Invariant Region

It is important to determine the invariant region since it describes the area where the system makes meaningful biological sense. This was done by assessing the nonnegativity of the solution.

### 3.4.2 Positivity of Solutions

We did this by assessing the nonnegativity of the solutions in the model, which shows our model was well-posed.

### 3.4.3 Boundedness of Solutions

The analysis aids in ensuring that the model is well-posed, significant, and realistic in representing the human population and bacteria population in the environment. The study applied the integration method and concluded that the model remains positive in the defined region.

### 3.4.4 Disease-Free Equilibrium

A system is said to be at Equilibrium when the rates of change with time are equal to zero. Therefore, we obtained our DFE of the system (1-5), by equating all the infectious classes to zero which resulted to  $E_0 = \frac{\lambda}{\mu}$ , where  $E_0$  is the disease-free equilibrium.

### 3.4.5 Basic Reproduction number ( $R_0$ )

We applied the next generation matrix to determine the basic reproduction number (Kanyi et al., 2021). We defined the non-negative matrix  $F$  which represented the new infections and non-singular matrix  $V$  which represented the transfer of infection from one compartment to another. Both Matrix  $F$  and Matrix  $V$  were evaluated at DFE. Thus, we had;

$F = \left[ \frac{\partial F_i E_0}{\partial x_j} \right]$ , and  $V = \left[ \frac{\partial V_i E_0}{\partial x_j} \right]$ . Where,  $i, j = 1, 2 \dots$  and  $E_0$  is the disease-free equilibrium. Thus, from the Matrix  $FV^{-1}$ , the reproduction number was given by the most dominant eigenvalue which was evaluated using Mathematica Software.

$$FV^{-1} = \left[ \frac{\partial F_i E_0}{\partial x_j} \right] \left[ \frac{\partial V_i E_0}{\partial x_j} \right]^{-1}$$

#### **3.4.6 Local Stability of Disease-Free Equilibrium Point**

When individuals in a given community move towards the direction of the equilibrium point, that situation is referred to as locally stable. We used the Routh-Hurwitz criteria to show the Local stability Wesley et al., (2010). Mathematica Software was used to calculate the characteristic equation and its coefficient. Lastly, we imposed the Routh-Hurwitz conditions for the locally asymptotically stability of the system.

#### **3.4.7 Global Stability of Disease-Free Equilibrium Point**

We used the Castillo-Chavez method to determine the necessary conditions for the global asymptotic stability of the DFE.

#### **3.4.8 Endemic Equilibrium Point**

The disease is said to be persistent at the endemic equilibrium point. The necessary condition for basic reproduction number was determined at EEP, which was used to predict the existence of EEP.

#### **3.4.9 Local Stability of EEP**

We applied the trace method of the Jacobian matrix to determine the Local stability of Endemic.

#### **3.4.10 Global Stability of EEP**

We used the Lyapunov function to determine the necessary conditions for the stability of the endemic equilibrium point.

### **3.5 Parameter Estimation**

The technique of determining parameters' unknown values from data is known as parameter estimation. The factors that determine a model's behavior are known as its parameters. The model can be used to make predictions about data that are not included in the original data set by estimating the values of these parameters.

### **3.6 Numerical simulation**

The numerical simulation was carried out to identify the role of the model parameters using MatLab2023a. The simulation was carried out using initial conditions and parameters values were obtained from the literature and then they were presented graphically.

## CHAPTER 4

### RESULTS AND INTERPRETATIONS

#### 4.1 Positivity and Boundedness of Solutions

Before we analyze the model (1)-(5), we need to verify that all the state variables remain positive implying that the solutions of the system of equations with positive initials conditions will remain positive for all  $t > 0$  and that the solutions are bounded for all  $t \geq 0$  in the positive region. We will establish conditions that ensure the positivity of solutions.

#### 4.2 Invariant Region

To determine the invariant region, we consider the total human population ( $N_h$ ), where  $N_h = S + I_h + I_e + R$ . Considering the model equations and then differentiating  $N_h$  with respect to  $t$  on both sides yields;

$$\frac{dN_h}{dt} = \frac{dS}{dt} + \frac{dI_h}{dt} + \frac{dI_e}{dt} + \frac{dR}{dt}. \quad (6)$$

Replacing the model equations (1)-(5) in equation (6), we have;

$$\begin{aligned} \frac{dN_h}{dt} = & \lambda - \rho(1 - \alpha)\beta_h S - (1 - \rho)\beta_e S(1 - \alpha) - \mu S + \omega R + \rho\beta_h S(1 - \alpha) - \mu I_h - \\ & \delta_1 I_h - \varepsilon_1 I_h + (1 - \alpha)(1 - \rho)\beta_e S - \mu I_e - \delta_2 I_e - \varepsilon_2 I_e + \varepsilon_1 I_h + \varepsilon_2 I_e - \mu R - \omega R, \end{aligned}$$

$$\frac{dN_h}{dt} = \lambda - \mu S - \mu I_h - \delta_1 I_h - \mu I_e - \delta_2 I_e - \mu R,$$

$$\frac{dN_h}{dt} = \lambda - \mu N_h - \delta I. \quad (7)$$

In mortality-free scenario due to typhoid fever disease,  $\delta = 0$ . Thus equation (7) becomes,

$$\frac{dN_h}{dt} \leq \lambda - \mu N_h. \quad (8)$$

Applying the separation of variables method in equation (8) we have;

$$\frac{dN_h}{dt} + \mu N_h \leq \lambda, \quad (9)$$

Multiplying all the terms of equation (9) by the integrating factor  $e^{\mu t}$  gives

$$\frac{dN_h}{dt} e^{\mu t} + \mu N_h e^{\mu t} \leq \lambda e^{\mu t} .$$

$= \frac{N_h(t)e^{\mu t}}{dt}$  by product rule. Thus it implies;

$$N_h(t)e^{\mu t} \leq \lambda e^{\mu t} dt \text{ thus, } N_h(t)e^{\mu t} \leq \int \lambda e^{\mu t} dt.$$

Therefore,  $N_h(t)e^{\mu t} \leq \frac{\lambda}{\mu}e^{\mu t} + c$  (10), where  $c$  is the constant of integration. Let  $N_h(0) = N_0$  be the initial conditions, then;

$$c \leq N_0 - \frac{\lambda}{\mu} \quad (11)$$

Substituting equation (11) in equation (10) we have;

$$N_h(t)e^{\mu t} \leq \frac{\lambda}{\mu}e^{\mu t} + N_0 - \frac{\lambda}{\mu}. \quad (12)$$

Dividing equation (12) all through by  $e^{\mu t}$  we have;

$$N_h(t) \leq \frac{\lambda}{\mu} + N_0e^{-\mu t} - \frac{\lambda}{\mu}e^{-\mu t}. \text{ Implying that;}$$

$$N_h(t) \leq \frac{\lambda}{\mu}(1 - e^{-\mu t}) + N_0e^{-\mu t}. \quad (13)$$

If  $N_0 \leq \frac{\lambda}{\mu}$  then, from equation (13) we have  $N_h(t) \leq \frac{\lambda}{\mu}$  which shows that the  $N_h(t)$  is bounded. Furthermore,  $\lim_{t \rightarrow \infty} \text{Sup} [N_h(t) \leq \frac{\lambda}{\mu}]$ . This concludes that the defined feasible region is positively invariant and attracting.

### 4.3 Positivity of Solutions.

To determine the positivity of solutions, we prove the following theorem;

#### Theorem 1

Let  $R = \{S, I_h, I_e, R, B\} \in R_+^5: S_0 > 0, I_{h_0} > 0, I_{e_0} > 0, R_0 > 0, B_0 > 0$ ; then the solutions of  $R = \{S, I_h, I_e, R, B\}$  are positive for all  $t \geq 0$ .

#### Proof

Let  $S, I_h, I_e, R$  and  $B$  be a solution of the system with non-negative initial conditions.

From the system of differential equations, we consider equation (1);

$$\frac{dS}{dt} = \lambda - [(\rho\beta_h + (1 - \rho)\beta_e)(1 - \alpha) + \mu]S + \omega R.$$

The first  $\lambda$ , and the last term  $\omega R$  are positive by inspection method.

$$\frac{dS(t)}{dt} \geq -[(\rho\beta_h + (1 - \rho)\beta_e)(1 - \alpha) + \mu]S(t),$$

$$\int \frac{dS(t)}{S(t)} \geq -\int_0^t [(\rho\beta_h + (1 - \rho)\beta_e)(1 - \alpha) + \mu] dt,$$

$$\ln S(t) \geq -\int_0^t [(\rho\beta_h + (1 - \rho)\beta_e)(1 - \alpha) + \mu] dt + c,$$

$$e^{\ln S(t)} \geq e^{-\int_0^t [(\rho\beta_h + (1 - \rho)\beta_e)(1 - \alpha) + \mu] dt} e^c,$$

$$S(t) \geq e^{-\int_0^t [(\rho\beta_h + (1-\rho)\beta_e)(1-\alpha) + \mu] dt} e^c. \quad (14)$$

Applying the initial condition, that is, we let  $t = 0$ ,

$$S(0) \geq e^c,$$

Therefore equation (14) becomes,

$$S(t) = S(0)e^{-\int_0^t [(\rho\beta_h + (1-\rho)\beta_e)(1-\alpha) + \mu] dt} \geq 0. \quad (15)$$

From equation (2),

$$\frac{dI_h}{dt} = \rho\beta_h(1-\alpha)S - (\mu + \delta_1 + \varepsilon_1)I_h.$$

The first term is positive by inspection.

$$\frac{dI_h(t)}{dt} \geq -(\mu + \delta_1 + \varepsilon_1)I_h(t),$$

$$\int \frac{dI_h(t)}{I_h(t)} \geq -\int_0^t (\mu + \delta_1 + \varepsilon_1) dt,$$

$$\ln I_h(t) \geq -\int_0^t (\mu + \delta_1 + \varepsilon_1) dt + c,$$

$$e^{\ln I_h(t)} \geq e^{-\int_0^t (\mu + \delta_1 + \varepsilon_1) dt} e^c,$$

$$I_h(t) = e^{-\int_0^t (\mu + \delta_1 + \varepsilon_1) dt} e^c. \quad (16)$$

Letting  $t = 0$ , equation (16) becomes,

$$I_h(0) = e^c.$$

Therefore,

$$I_h(t) = I_h(0) e^{-\int_0^t (\mu + \delta_1 + \varepsilon_1) dt} \geq 0. \quad (17)$$

From equation (3),

$$\frac{dI_e}{dt} = \rho\beta_h(1-\alpha)(1-\rho)S - (\mu + \delta_2 + \varepsilon_2)I_e.$$

The first term is positive by inspection.

$$\frac{dI_e(t)}{dt} \geq -(\mu + \delta_2 + \varepsilon_2)I_e(t),$$

$$\int \frac{dI_e(t)}{I_e(t)} \geq -\int_0^t (\mu + \delta_2 + \varepsilon_2) dt,$$

$$\ln I_e(t) \geq -\int_0^t (\mu + \delta_2 + \varepsilon_2) dt + c,$$

$$e^{\ln I_e(t)} \geq e^{-\int_0^t (\mu + \delta_2 + \varepsilon_2) dt} e^c,$$

$$I_e(t) = e^{-\int_0^t (\mu + \delta_2 + \varepsilon_2) dt} e^c. \quad (18)$$

Letting  $t = 0$ , equation (18) becomes,

$$I_e(0) = e^c.$$

Therefore,

$$I_e(t) = I_e(0) e^{-\int_0^t (\mu + \delta_2 + \varepsilon_2) dt} \geq 0.$$

From equation (4),

$$\frac{dR}{dt} = \varepsilon_1 I_h + \varepsilon_2 I_e - (\mu + \omega)R.$$

The first and the second term,  $\varepsilon_1 I_h$ ,  $\varepsilon_2 I_e$  are positive by inspection.

$$\frac{dR(t)}{dt} \geq -(\mu + \omega)R(t),$$

$$\int \frac{dR(t)}{R(t)} \geq -\int_0^t (\mu + \omega) dt,$$

$$\ln R(t) \geq -\int_0^t (\mu + \omega) dt + c,$$

$$e^{\ln R(t)} \geq e^{-\int_0^t (\mu + \omega) dt} e^c,$$

$$R(t) = e^{-\int_0^t (\mu + \omega) dt} e^c. \quad (19)$$

Letting  $t = 0$ , equation (19) becomes,

$$R(0) = e^c.$$

Therefore,

$$R(t) = R(0) e^{-\int_0^t (\mu + \omega) dt} \geq 0. \quad (20)$$

Considering equation (5),

$$\frac{dB}{dt} = b + \eta_1 I_h + \eta_2 I_e - \tau B,$$

$$\frac{dB}{dt} = rB \left(1 - \frac{B}{K}\right) + \eta_1 I_h + \eta_2 I_e - \tau B.$$

The term  $rB \left(1 - \frac{B}{K}\right) + \eta_1 I_h + \eta_2 I_e$  is positive by inspection.

$$\frac{dB(t)}{dt} \geq -\tau B(t),$$

$$\int \frac{dB(t)}{B(t)} \geq - \int_0^t \tau dt,$$

$$\ln B(t) \geq - \int_0^t \tau dt + c,$$

$$e^{\ln B(t)} \geq e^{- \int_0^t \tau dt} e^c,$$

$$B(t) \geq e^{- \int_0^t \tau dt} e^c. \quad (20)$$

Letting  $t = 0$ , equation (20) becomes,

$$B(0) = e^c.$$

Therefore,

$$B(t) = B(0) e^{- \int_0^t \tau dt} \geq 0. \quad (21)$$

This concludes the proof of the theorem. Therefore, the solutions of the model are positive.

#### 4.4 Boundedness of Solutions.

We partitioned the model into two sections which comprises, population of humans  $T_H$  and the bacteria intensity in the environment  $T_B$  such that;

$$T_H = (S_h(t), I_h(t), I_e(t), R_h(t)) \in \mathbb{R}_+^4 : S_h + I_h + I_e + R_h = N_h, \quad \text{and} \quad T_B = B(t) \in \mathbb{R}_+^1 \text{ respectively.}$$

We consider boundedness of solutions of system (1) to (4) at the time  $t$  given as

$$N_h(t) = S_h(t) + I_h(t) + I_e(t) + R_h(t). \quad (22)$$

Differentiating equation (22) with respect to  $t$  yields;

$$\frac{dN_h}{dt} = \frac{dS_h}{dt} + \frac{dI_h}{dt} + \frac{dI_e}{dt} + \frac{dR_h}{dt}. \quad (23)$$

Substituting equations (1-4) in equation (22) we have;

$$\begin{aligned} \frac{dN_h}{dt} = & \lambda - [(\rho\beta_h + (1 - \rho)\beta_e)(1 - \alpha) + \mu]S + \omega R + \rho\beta_h(1 - \alpha)S - \\ & (\mu + \delta_1 + \varepsilon_1)I_h + \rho\beta_h(1 - \alpha)(1 - \rho)S - (\mu + \delta_2 + \varepsilon_2)I_e + \varepsilon_1 I_h + \\ & \varepsilon_2 I_e - (\mu + \omega)R, \end{aligned}$$

$$\frac{dN_h}{dt} = \lambda - \mu N_h - \delta I. \quad (24)$$

In absence of no infectious human with typhoid fever ( $\delta = 0$ ), equation (13) becomes;

$$\frac{dN_h}{dt} \leq \lambda - \mu N_h(t). \quad (25)$$

Applying the method of separation of variables of inequality, we have;

$$-\frac{1}{\mu} \ln(\lambda - \mu N_h(t)) \leq t + c,$$

$$\lambda - \mu N_h(t) \geq A e^{-\mu t}. \quad (26)$$

Solving (26) and evaluating as  $t \rightarrow \infty$ , we have;

$$\lim_{t \rightarrow \infty} N_h(t) = \frac{\lambda}{\mu}. \quad (27)$$

Implying that,

$$0 \leq N_h(t) \leq \frac{\lambda}{\mu}. \quad (28)$$

Therefore, the model is bounded in the domain.

$$T_H = (S_h(t), I_h(t), I_e(t), R_h(t)) \in \mathbb{R}_+^4: 0 \leq N_h(t) \leq \frac{\lambda}{\mu}.$$

We then consider the boundedness of solution for the bacteria concentration at time  $t$  from (5), we have;

$$\frac{dB}{dt} = b + \eta_1 I_h + \eta_2 I_e - \tau B,$$

$$\frac{dB}{dt} + \tau B = b + \eta_1 I_h + \eta_2 I_e. \quad (29)$$

Let  $M = b + \eta_1 I_h + \eta_2 I_e$ , which is the rate at which bacteria from infectious groups are recruited. Next, we obtain a differential inequality;

$$\frac{dB}{dt} + \tau B \leq M. \quad (30)$$

Using the integration factor method;

$$I.F = e^{\int \tau dt},$$

$$I.F = e^{\tau t}. \quad (31)$$

Multiplying (30) by (31) on both sides we have;

$$e^{\tau t} B' + e^{\tau t} \tau B = M e^{\tau t},$$

$$B \leq \frac{M}{\tau} + C e^{-\tau t}. \quad (32)$$

Where  $C$  is a constant of integration. Thus, as  $t \rightarrow \infty$ , we have,

$$\lim_{t \rightarrow \infty} B(t) = \frac{M}{\tau}. \text{ Which implies that,}$$

$$0 \leq B(t) \leq \frac{M}{\tau}. \quad (33)$$

$$T_B = B(t) \in \mathbb{R}_+^1: 0 \leq B(t) \leq \frac{M}{\tau}.$$

Thus, the model is bounded as;

$$R = \left[ (S_h, I_h, I_e, R_h, B) \geq 0: N_h(t) \leq \frac{\lambda}{\mu}; B(t) \leq \frac{M}{\tau} \right].$$

#### 4.5 Disease-Free Equilibrium (DFE)

To compute the DFE, we set the right-hand side of the model equations (1)- (5) to zero.

$$\lambda - [(\rho\beta_h + (1 - \rho)\beta_e)(1 - \alpha) + \mu]S + \omega R = 0. \quad (34)$$

$$\left. \begin{aligned} \rho\beta_h(1 - \alpha)S - (\mu + \delta_1 + \varepsilon_1)I_h &= 0 \\ \rho\beta_h(1 - \alpha)(1 - \rho)S - (\mu + \delta_2 + \varepsilon_2)I_e &= 0 \\ \varepsilon_1 I_h + \varepsilon_2 I_e - (\mu + \omega)R &= 0 \\ rB \left(1 - \frac{B}{K}\right) + \eta_1 I_h + \eta_2 I_e - \tau B &= 0 \end{aligned} \right\}. \quad (35)$$

Furthermore, we set  $I_h = I_e = B = 0$  since we assume that there is no infection in the community or the disease is not detected in the population. Consequently, equation (34) reduces to;

$$\lambda - \mu S = 0,$$

$$S = \frac{\lambda}{\mu}.$$

On solving equation (35), the result is zero. Thus, the disease-free equilibrium becomes;

$$E_0 = \left( \frac{\lambda}{\mu}, 0, 0, 0, 0 \right). \quad (36)$$

#### 4.6 The Basic Reproduction Number ( $R_0$ )

The reproduction number  $R_0$  is the mean number of secondary infections caused by contagious individual in his or her entire duration of infectiousness in a completely susceptible population. In this study, we compute the  $R_0$  using the next generation matrix method described in Kanyi et al., (2021). The reproduction number is a key quantity measure in the disease epidemiology as it is a determining factor of whether the disease persists or die out in a given population. When  $R_0 > 1$ , it indicates that each infected person is typically causing more than one secondary infection thus the epidemic the disease invades the population. In contrast, the disease is likely to die out when  $R_0 < 1$ , since an infected individual typically infects fewer people. We define matrix  $FV^{-1}$  as ;

$$FV^{-1} = \left[ \frac{\partial F_i E_0}{\partial x_j} \right] \left[ \frac{\partial V_i E_0}{\partial x_j} \right]^{-1},$$

where matrix  $F_i$  represents the rate of appearances of new infections in compartment  $i$ . Matrix  $V_i$  represent the transfer of infections from one compartment  $i$  to another and  $E_0$  is the disease-free equilibrium and  $i, j = 1, 2, 3 \dots$

$$F_i = \begin{bmatrix} \rho \beta_h (1 - \alpha) S \\ (1 - \rho)(1 - \alpha) \beta_h S \\ 0 \end{bmatrix}, \text{ where; } \beta_h = \frac{(1 - \psi_f) C_h (\eta_1 I_h + \eta_2 I_e)}{N_h}, \quad \beta_e = \frac{C_e (1 - \psi_f) B}{K + B} \text{ and}$$

$S = N_h = \frac{\lambda}{\mu}$  at the disease free equilibrium.

Therefore, infection matrix  $F_i$  and transition matrix  $V_i$  are given as follows;

$$F_i = \begin{pmatrix} \rho(1 - \alpha)(1 - \psi_f) C_h (\eta_1 I_h + \eta_2 I_e) \\ \frac{\rho(1 - \psi_f) C_e B (1 - \alpha) \lambda}{(K + B) \mu} \\ 0 \end{pmatrix},$$

$$V_i = \begin{pmatrix} (\mu + \delta_1 + \varepsilon_1) I_h \\ (\mu + \delta_2 + \varepsilon_2) I_e \\ (\tau - r) B - \eta_1 I_h - \eta_2 I_e \end{pmatrix}.$$

Differentiating  $F_i$  and  $V_i$  with respect to  $I_h$ ,  $I_e$  and  $B$  at the disease-free equilibrium  $E_0$  we obtain matrix  $F$  and  $V$  as;

$$F = \begin{pmatrix} \rho(1 - \psi_f) C_h (\eta_1) (1 - \alpha) & \rho(1 - \psi_f) C_h (\eta_2) (1 - \alpha) & 0 \\ 0 & 0 & \frac{\rho(1 - \psi_f) C_e (1 - \alpha) \lambda}{K \mu} \\ 0 & 0 & 0 \end{pmatrix},$$

$$V = \begin{pmatrix} \mu + \delta_1 + \varepsilon_1 & 0 & 0 \\ 0 & \mu + \delta_2 + \varepsilon_2 & 0 \\ -\eta_1 & -\eta_2 & \tau - r \end{pmatrix},$$

The inverse of matrix  $V$ , denoted  $V^{-1}$  is given as

$$V^{-1} = \begin{pmatrix} \frac{1}{\mu + \delta_1 + \varepsilon_1} & 0 & 0 \\ 0 & \frac{1}{\mu + \delta_2 + \varepsilon_2} & 0 \\ \frac{\eta_1}{(\mu + \delta_1 + \varepsilon_1)(\tau - r)} & \frac{\eta_2}{(\mu + \delta_2 + \varepsilon_2)(\tau - r)} & \frac{1}{\tau - r} \end{pmatrix}.$$

Computing  $FV^{-1}$  we have,

$$\begin{aligned}
\mathbf{FV}^{-1} &= \\
&\begin{pmatrix} \rho(1-\psi_f)c_h(\eta_1)(1-\alpha) & \rho(1-\psi_f)c_h(\eta_2)(1-\alpha) & 0 \\ 0 & 0 & \frac{\rho(1-\psi_f)c_e(1-\alpha)\lambda}{K\mu} \\ 0 & 0 & 0 \end{pmatrix} X \begin{pmatrix} \frac{1}{\mu+\delta_1+\varepsilon_1} & 0 & 0 \\ 0 & \frac{1}{\mu+\delta_2+\varepsilon_2} & 0 \\ \frac{\eta_1}{(\mu+\delta_1+\varepsilon_1)(\tau-r)} & \frac{\eta_2}{(\mu+\delta_2+\varepsilon_2)(\tau-r)} & \frac{1}{\tau-r} \end{pmatrix} \\
\mathbf{FV}^{-1} &= \begin{bmatrix} \frac{\rho(1-\psi_f)c_h(\eta_1)(1-\alpha)}{\mu+\delta_1+\varepsilon_1} & \frac{\rho(1-\psi_f)c_h(\eta_2)(1-\alpha)}{\mu+\delta_2+\varepsilon_2} & 0 \\ \frac{(1-\alpha)(1-\rho)(1-\psi_f)c_e\eta_1\lambda}{(\mu+\delta_1+\varepsilon_1)(\tau-r)\mu} & \frac{(1-\alpha)(1-\rho)(1-\psi_f)c_e\eta_2\lambda}{(\mu+\delta_2+\varepsilon_2)(\tau-r)\mu} & \frac{(1-\alpha)(1-\rho)(1-\psi_f)c_e\lambda}{K(\tau-r)\mu} \\ 0 & 0 & 0 \end{bmatrix}.
\end{aligned}$$

The basic reproduction number,  $R_0$ , is the spectral radius of  $\mathbf{FV}^{-1}$  which is given by the dominant eigenvalue value of the next generation matrix. To find the eigenvalues, we first consider the following conventions to simplify the expressions in the matrix  $\mathbf{FV}^{-1}$ .

$$\begin{aligned}
R_1 &= \frac{\rho(1-\psi_f)c_h(\eta_1)(1-\alpha)}{\mu+\delta_1+\varepsilon_1}, \\
R_2 &= \frac{\rho(1-\psi_f)c_h(\eta_2)(1-\alpha)}{\mu+\delta_2+\varepsilon_2}, \\
R_3 &= \frac{(1-\alpha)(1-\rho)(1-\psi_f)c_e\eta_1\lambda}{(\mu+\delta_1+\varepsilon_1)(\tau-r)\mu}, \\
R_4 &= \frac{(1-\alpha)(1-\rho)(1-\psi_f)c_e\eta_2\lambda}{(\mu+\delta_2+\varepsilon_2)(\tau-r)\mu}, \\
R_5 &= \frac{(1-\alpha)(1-\rho)(1-\psi_f)c_e\lambda}{K(\tau-r)\mu}.
\end{aligned}$$

Computing the eigenvalues yields the following;

$$\begin{aligned}
\lambda_1 &= 0. \\
\lambda_2 &= \frac{1}{2}(R_4 + R_1 - \sqrt{(R_4 - R_1)^2 + 4R_2R_3}). \\
\lambda_3 &= \frac{1}{2}(R_4 + R_1 + \sqrt{(R_4 - R_1)^2 + 4R_2R_3}).
\end{aligned}$$

Where  $\lambda_3$  is the dominant eigenvalue with  $R_4 \geq R_1$ . The reproduction number  $R_0$  for typhoid fever model system described in equations (1)-(5) is given in equation (37) as;

$$R_0 = \frac{1}{2}(R_4 + R_1 + \sqrt{(R_4 - R_1)^2 + 4R_2R_3}). \quad (37)$$

$R_1$  and  $R_2$  represent the mean number of newly infected individuals through direct mode of typhoid fever transmission whereas  $R_5$  represents the average number of

newly infected individuals through indirect modes.  $R_3$  and  $R_4$  represent the average number of newly infected individuals through both direct and indirect modes. This implies that  $R_1$ , represents the average number of newly infected individuals resulting from interactions between susceptible population and infected population  $I_h$  only whereas  $R_2$  stems from interplay between susceptible population and infected population  $I_e$  only.  $R_5$  represents average number of newly infected population when interaction only occurs between a susceptible population and contaminated environment.  $R_3$  stems from interactions between susceptible population and infected population  $I_h$  as well as contaminated environment. Similarly,  $R_4$  results from interactions between a susceptible population and infected population  $I_e$  as well as contaminated environment.

#### 4.7 Local Stability of Disease-Free Equilibrium (DFE)

##### Theorem 2.

The DFE of the model (1)-(5) is locally asymptotically stable if  $R_0 < 1$ .

##### Proof.

We apply the Routh Hurwitz Criterion Wesley et al., (2010), which states that given a polynomial of degree 3 that is,  $P(\lambda) = \lambda^3 + a_1\lambda^2 + a_2\lambda + a_3 = 0$  the corresponding Hurwitz Matrix is given as;

$$Q = \begin{vmatrix} a_1 & 1 & 0 \\ a_3 & a_2 & a_1 \\ 0 & 0 & a_3 \end{vmatrix}$$

To verify if the disease-free equilibrium point is locally stable using the Routh Hurwith criterion, we need to show that the determinant,  $\det(Q) = a_3(a_1a_2 - a_3) > 0$ ,

$a_1 > 0, a_3 > 0$  and  $a_1a_2 > a_3$ .

To get Matrix  $Q$  we subtract Matrix  $F$  and Matrix  $V$ , that is;

$$F - V = \begin{pmatrix} \rho(1 - \psi_f)C_h(\eta_1)(1 - \alpha) & \rho(1 - \psi_f)C_h(\eta_2)(1 - \alpha) & 0 \\ 0 & 0 & \frac{\rho(1 - \psi_f)C_e(1 - \alpha)\lambda}{K\mu} \\ 0 & 0 & 0 \end{pmatrix} - \begin{pmatrix} \mu + \delta_1 + \varepsilon_1 & 0 & 0 \\ 0 & \mu + \delta_2 + \varepsilon_2 & 0 \\ -\eta_1 & -\eta_2 & \tau - r \end{pmatrix},$$

$$F - V = \begin{pmatrix} a - d & b & 0 \\ 0 & -e & c \\ -f & -g & -h \end{pmatrix}.$$

To find the characteristic equation we find;

$$|(F - V) - \lambda I| = 0.$$

$$(F - V) - \lambda I = \begin{bmatrix} a-d & b & 0 \\ 0 & -e & c \\ -f & -g & -h \end{bmatrix} - \begin{bmatrix} \lambda & 0 & 0 \\ 0 & \lambda & 0 \\ 0 & 0 & \lambda \end{bmatrix} = \begin{bmatrix} a-d-\lambda & b & 0 \\ 0 & -e-\lambda & c \\ -f & -g & -h-\lambda \end{bmatrix},$$

$$|(F - V) - \lambda I| = \begin{vmatrix} a-d-\lambda & b & 0 \\ 0 & -e-\lambda & c \\ -f & -g & -h-\lambda \end{vmatrix} = 0,$$

Thus, we have,

$$a-d-\lambda \begin{vmatrix} -e-\lambda & c \\ -g & -h-\lambda \end{vmatrix} - b \begin{vmatrix} 0 & c \\ -f & -h-\lambda \end{vmatrix} + 0 \begin{vmatrix} 0 & -e-\lambda \\ -f & -g \end{vmatrix} = 0.$$

Thus, the characteristic equation becomes,

$$P(\lambda) = -\lambda^3 + (a-d-e-h)\lambda^2 + (ae+ah-de-dh-eh-cg)\lambda + aeh+acg-deh-dcg-bcf = 0.$$

From the Routh Hurwitz stability criterion, the characteristic equation becomes,

$$P(\lambda) = \lambda^3 - (a-d-e-h)\lambda^2 - (ae+ah-de-dh-eh-cg)\lambda - aeh-acg+deh+dcg+bcf = 0.$$

Thus, comparing this characteristic equation with the general form of Routh Hurwitz stability criterion, we have,

$$a_1 = d + e + h - a,$$

$$a_2 = de + dh + eh + cg - ae - ah,$$

$$a_3 = deh + dcg + bcf - aeh - acg.$$

Thus, the Hurwitz matrix becomes,

$$Q = \begin{vmatrix} d+e+h-a & 1 & 0 \\ deh+dcg+bcf-aeh-acg & de+dh+eh+cg-ae-ah & d+e+h-a \\ 0 & 0 & deh+dcg+bcf-aeh-acg \end{vmatrix},$$

$$\det Q = deh + dcg + bcf - aeh - acg((d + e + h - a)(de + dh + eh + cg - ae - ah) - (deh + dcg + bcf - aeh - acg)) > 0.$$

Therefore, according to Routh Hurwitz, the following conditions are satisfied.

$$a_1 = d + e + h > a,$$

$$a_3 = deh + dcg + bcf > aeh + acg,$$

$$a_1 a_2 = ea^2 + a^2 h + 2ed^2 + d^2 h + 3edh + ecg + dh^2 + eh^2 + cdg - acg - 2ead - 2adh - 3eah - ah^2 - ea^2 > a_3.$$

Thus, since  $\det Q > 0, a_1 > 0, a_3 > 0$ , and,  $a_1 a_2 > a_3$  then the disease-free equilibrium point is locally stable.

Where;

$$a = \rho(1 - \psi_f)C_h(\eta_1)(1 - \alpha),$$

$$b = \rho(1 - \psi_f)C_h(\eta_2)(1 - \alpha),$$

$$c = \frac{\rho(1-\psi_f)C_e(1-\alpha)\lambda}{K\mu},$$

$$d = \mu + \delta_1 + \varepsilon_1,$$

$$e = \mu + \delta_2 + \varepsilon_2,$$

$$f = \eta_1,$$

$$g = \eta_2,$$

$$h = \tau - r.$$

#### 4.8 Global Stability of the DFE

To determine the global stability of the DFE, the Castillo-Chavez method is applied Castillo-chavez, (2001). We consider the following theorem;

##### Theorem 3

The disease-free equilibrium of the model (1) – (5) is globally asymptotically stable if  $R_0 \leq 1$ .

##### Proof

Considering the theorem above, the system of equation (1)-(5) reduces to;

$$\begin{cases} \frac{dX}{dt} = F(X, Z) \\ \frac{dZ}{dt} = G(X, Z), G(X, 0) = 0 \end{cases}$$

Where  $X$  represent the population not infected while  $Z$  represent the infected population.

And  $E_0 = (X, 0), P = (X^*, 0) = \left(\frac{\lambda}{\mu}, 0, 0, 0, 0\right)$  represents the disease-free equilibrium state of the system.

To guarantee the global asymptotic stability, the following conditions must also satisfy;

(H1):  $\frac{dX}{dt} = F(X^*, 0), X^*$  is globally asymptotic stable.

(H2):  $G(X, Z) = AI - G(X, 0) \geq 0$  for  $(X, Z) \in \mathbb{R}_+^2$  where  $A=D_1G(X^*, 0)$  is the Metzler matrix that is, the domain where the model is well-posed and makes biological

sense is the non-negative off diagonal element of  $A$ . And this implies that the fixed point  $E_0 = (X^*, 0)$  has a global asymptotic stability point of the model provided  $R_0 < 1$ . Thus, for the condition (H1) to be satisfied we have;

$$F(X, 0) = \begin{pmatrix} \lambda - [(\rho\beta_h + (1 - \rho)\beta_e)(1 - \alpha) + \mu]S + \omega R \\ \varepsilon_1 I_h + \varepsilon_2 I_e - (\mu + \omega)R \end{pmatrix},$$

For the equilibrium state  $E_0 = (X^*, 0)$  the systems yield the following,

$$\frac{dX}{dt} = \lambda - [(\rho\beta_h + (1 - \rho)\beta_e)(1 - \alpha) + \mu]S + \omega R,$$

$$\frac{dX}{dt} = \varepsilon_1 I_h + \varepsilon_2 I_e - (\mu + \omega)R.$$

Which implies that,

$$F(X, 0) = \begin{pmatrix} -[(\rho\beta_h + (1 - \rho)\beta_e)(1 - \alpha) + \mu] & \omega \\ 0 & -(\mu + \omega) \end{pmatrix}.$$

Letting  $w = (\rho\beta_h + (1 - \rho)\beta_e)(1 - \alpha)$  and determining the characteristic polynomial, we apply the following;

$$F(X, 0) - \lambda I = \begin{pmatrix} -(w + \mu) & \omega \\ 0 & -(\mu + \omega) \end{pmatrix} - \begin{pmatrix} \lambda & 0 \\ 0 & \lambda \end{pmatrix} = 0.$$

Implying that,

$$\begin{vmatrix} -(w + \mu) - \lambda & \omega \\ 0 & -(\mu + \omega) - \lambda \end{vmatrix} = 0.$$

Thus, the characteristic equation of the polynomial becomes;

$$\lambda^2 + (3\omega + w)\lambda + 2(w + \omega)\omega = 0. \quad (38)$$

According to the Routh-Hurwitz criterion, solutions to the characteristic polynomial contain negative real components as all of the characteristic polynomials in equation (38) are non-negative. Thus, suggests that the real parts of the eigenvalues are negative. As a result,  $X^*$  is globally asymptotic stable.

Furthermore, for (H2) to be satisfied, that is:  $G(X, Z) = AI - G(X, 0)$

$$G(X, Z) = \begin{pmatrix} -(\mu + \delta_1 + \varepsilon_1) & 0 & 0 \\ 0 & -(\mu + \delta_2 + \varepsilon_2) & 0 \\ \eta_1 & \eta_2 & r - \tau \end{pmatrix}.$$

Thus,  $G(X, Z) = AI - G(X, 0)$  becomes;

$$\begin{pmatrix} -(\mu + \delta_1 + \varepsilon_1) & 0 & 0 \\ 0 & -(\mu + \delta_2 + \varepsilon_2) & 0 \\ \eta_1 & \eta_2 & r - \tau \end{pmatrix} \begin{pmatrix} I_h \\ I_e \\ B \end{pmatrix} - \begin{pmatrix} \rho\beta_h(1-\alpha)S \\ (1-\rho)\beta_e(1-\alpha)S \\ 0 \end{pmatrix}.$$

Since  $A$  is a Metzler matrix, and that as  $t \rightarrow \infty$ ,  $(I_h, I_e, B) \rightarrow (0,0)$ . Therefore,  $F(X, Z) \geq 0$  and since the two conditions are satisfied the disease-free equilibrium is globally asymptotically stable in  $\mathbb{R}$ .

#### 4.9 The Endemic Equilibrium Point.

We consider the following Lemma;

##### Lemma 4.

For  $R_0 > 1$ , there exists a unique equilibrium point at  $E^*$  otherwise it does not exist.

Proof.

To measure the endemic equilibrium point that is  $E^* = (S_h^*, I_h^*, I_e^*, R^*, B^*)$ , we equate the systems of differential equation for the states  $S, I_h, I_e, R, B$  to zero to estimate the endemic equilibrium points for both the human and bacteria populations.

Determining the endemic equilibrium for the human population that is,  $E_h^* = (S^*, I_h^*, I_e^*, R^*)$ , we let,

$$a_1 = \rho(1 - \alpha),$$

$$a_2 = (1 - \rho)(1 - \alpha),$$

$$a_3 = \mu + \delta_1 + \varepsilon_1,$$

$$a_4 = \mu + \delta_2 + \varepsilon_2.$$

And let  $\beta_h^*$  and  $\beta_e^*$  be equilibrium points such that;

$$\beta_h^* \leq \frac{(1-\psi_f)(\eta_1 I_h^* + \eta_2 I_e^*)}{N_h^*},$$

$$\beta_e^* \leq \frac{C_e(1-\psi_f)B^*}{K+B^*}.$$

Thus, computing the endemic equilibrium for the human population yields;

$$S_h^* \approx \frac{a_2 a_3 a_4 \lambda}{a_1 a_2 a_3 a_4 \beta_h^* - a_1 a_3 \omega \beta_h^* \varepsilon_1 + a_2^2 a_3 a_4 \beta_e^* - a_2^2 \omega \beta_e^* \varepsilon_2 + a_2 a_3 a_4 \mu} > 0,$$

$$I_h^* \approx \frac{\lambda(a_1 a_3 \beta_h^* \varepsilon_1) + a_2^2 \beta_e^* \varepsilon_2}{a_1 a_2 a_3 a_4 \beta_h^* - a_1 a_3 \omega \beta_h^* \varepsilon_1 + a_2^2 a_3 a_4 \beta_e^* - a_2^2 \omega \beta_e^* \varepsilon_2 + a_2 a_3 a_4 \mu} > 0,$$

$$I_e^* \approx \frac{(a_1 a_3 \beta_h^* a_4) \lambda}{a_1 a_2 a_3 a_4 \beta_h^* - a_1 a_3 \omega \beta_h^* \varepsilon_1 + a_2^2 a_3 a_4 \beta_e^* - a_2^2 \omega \beta_e^* \varepsilon_2 + a_2 a_3 a_4 \mu} > 0,$$

$$R_h^* \approx \frac{a_2^2 \beta_e^* a_4 \lambda}{a_1 a_2 a_3 a_4 \beta_h^* - a_1 a_3 \omega \beta_h^* \varepsilon_1 + a_2^2 a_3 a_4 \beta_e^* - a_2^2 \omega \beta_e^* \varepsilon_2 + a_2 a_3 a_4 \mu} > 0.$$

Calculating the endemic equilibrium for the bacteria population we let  $b^*$  be an endemic equilibrium point such that;

$$b^* \leq rB^* \left(1 - \frac{B^*}{K}\right).$$

Therefore,

$$b^* + \eta_1 I_h^* + \eta_2 I_e^* - \tau B \geq 0,$$

$$rB(K - B) + \eta_1 K I_h^* + \eta_2 K I_e^* - \tau B K \geq 0,$$

$$K r B - r B^2 - \tau B K + \bar{\eta} K (I_h^* + I_e^*) \geq 0.$$

$$-r B^2 + B K (r - \tau) + \bar{\eta} K (I_h^* + I_e^*) \geq 0. \quad (39)$$

Let,

$$q_1 = K(r - \tau),$$

$$q_2 = \bar{\eta} K (I_h^* + I_e^*).$$

Solving the quadratic equation given in (39), the endemic equilibrium point for the bacteria population is approximated as follows;

$$B^* \leq \frac{q_1 + \sqrt{q_1^2 + 4r q_2}}{2r}$$

## 5.0 Global Stability of Endemic Equilibrium

To study the global asymptotic stability of the endemic equilibrium point, we apply the LaSalle's invariance principle.

Theorem 5.

The endemic equilibrium point  $E^*$  of a system is globally asymptotically stable when  $R_0 > 1$ .

Proof.

We employ the LaSalle's invariance principle to prove the global stability of the endemic equilibrium point. We use the following Lyapunov function.

$$V(S, I_h, I_e, R, B) \leq \left(S - S^* + S^* \ln \frac{S}{S^*}\right) + \left(I_h - I_h^* + I_h^* \ln \frac{I_h}{I_h^*}\right) + \left(I_e - I_e^* + I_e^* \ln \frac{I_e}{I_e^*}\right) + \left(R - R^* + R^* \ln \frac{R}{R^*}\right) + \left(B - B^* + B^* \ln \frac{B}{B^*}\right).$$

Differentiating  $V$  with respect to  $t$  we have;

$$\frac{dV}{dt} \leq \left(1 - \frac{S^*}{S}\right) \frac{dS}{dt} + \left(1 - \frac{I_h^*}{I_h}\right) \frac{dI_h}{dt} + \left(1 - \frac{I_e^*}{I_e}\right) \frac{dI_e}{dt} + \left(1 - \frac{R^*}{R}\right) \frac{dR}{dt} + \left(1 - \frac{B^*}{B}\right) \frac{dB}{dt}. \quad (40)$$

Replacing the values of  $\frac{dS}{dt}, \frac{dI_h}{dt}, \frac{dI_e}{dt}, \frac{dR}{dt}, \frac{dB}{dt}$  in equation (40) we obtain;

$$\begin{aligned} \frac{dV}{dt} \leq & \left(1 - \frac{S^*}{S}\right) (\lambda - [(\rho\beta_h + (1 - \rho)\beta_e)(1 - \alpha) + \mu]S + \omega R) + \left(1 - \frac{I_h^*}{I_h}\right) (\rho\beta_h(1 - \alpha)S - (\mu + \delta_1 + \varepsilon_1)I_h) + \left(1 - \frac{I_e^*}{I_e}\right) (\rho\beta_h(1 - \alpha)(1 - \rho)S - \\ & (\mu + \delta_2 + \varepsilon_2)I_e) + \left(1 - \frac{R^*}{R}\right) (\varepsilon_1 I_h + \varepsilon_2 I_e - (\mu + \omega)R) + \left(1 - \frac{B^*}{B}\right) \left(rB \left(1 - \frac{B}{K}\right) + \eta_1 I_h + \eta_2 I_e - \tau B\right). \end{aligned}$$

Which implies,

$$\begin{aligned} \frac{dV}{dt} \leq & \lambda + (\rho\beta_h(1 - \alpha) + (1 - \rho)(1 - \alpha)\beta_e + \mu)S^* + (\mu + \delta_1 + \varepsilon_1)I_h^* + (\mu + \delta_2 + \\ & \varepsilon_2)I_e^* + \varepsilon_1 I_h + \varepsilon_2 I_e + (\mu + \omega)R^* + \left(rB \left(1 - \frac{B}{K}\right) + \eta_1 I_h + \eta_2 I_e\right) - (\lambda + \\ & \omega R) \frac{S^*}{S} - (\mu + \delta_1 + \varepsilon_1)I_h - (\rho\beta_h(1 - \alpha)S) \frac{I_h^*}{I_h} - (\mu + \delta_2 + \varepsilon_2)I_e - (1 - \rho)(1 - \\ & \alpha)\beta_e S \frac{I_e^*}{I_e} - \mu R - (\varepsilon_1 I_h + \varepsilon_2 I_e) \frac{R^*}{R} - \left(rB \left(1 - \frac{B}{K}\right)\right) \frac{B^*}{B} - (\eta_1 I_h + \eta_2 I_e) \frac{B^*}{B}. \end{aligned}$$

Setting  $Q$  to represent the positive terms and  $W$  to represent the negative terms we have;

$$\frac{dV}{dt} \leq Q - W.$$

If  $Q < W$ , then  $\frac{dV}{dt} \leq 0$ ;

Note that,  $\frac{dV}{dt} \leq 0$  if and only if  $S = S^*, I_h = I_h^*, I_e = I_e^*, R = R^*, B = B^*$ . Thus, the largest compact invariant set in  $(S^*, I_h^*, I_e^*, R^*, B^*) \in \mathbb{R}_+^5$ :  $\frac{dV}{dt} \leq 0$  is the singleton  $E^*$  where  $E^*$  is the endemic equilibrium of the system (1)-(5). From the Lassaile's invariant principle, it shows that  $E^*$  is globally asymptotically stable  $\mathbb{R}_+^5$  if  $Q < W$ .

## 6.0 Numerical Simulation

In this study the main objective is to model transmission dynamics of typhoid fever disease, through direct and indirect modes. The aim is to analyze what happens to the system when control measures like vaccination, proper sanitation and human influence (fear) are effective or not. Additionally, we want to investigate the role of fear in the whole population. Thus, various graphical representations on the model have been generated using MATLAB R2023a Version which supports our analytical results.

Since most parameters values were not readily available, we picked the values from various sources and estimated some values as shown.

## 6.1 Parameter Estimation

This section outlines how the initial data and parameter values used for the model simulations were obtained. We formulated the model using demographic data from Kisii County in Kenya because most parameter values were estimated from a typhoid fever study Chamuchi et al., (2014) conducted there. The model can be applicable to various regions that share similar dynamics as this study, provided they fall within the parameter range of this research. Other parameter values were obtained from the weekly bulletin on typhoid fever outbreaks (WHO, 2023). Using demographic data from Kisii town in Kenya, we estimated the initial susceptible population to be approximately 130,000 (Chamuchi et al., 2014). Additionally, we used the Kenyan demographic data to calculate parameter values for recruitment and death rates. The average lifespan of a Kenyan is 67 years (Njenga & Kipchirchir, 2024). To estimate the death rate, we shall take the reciprocal of the average life expectancy, that is,  $\mu = \frac{1}{67} = 0.01493$ . In 2023, approximately 4% of deaths were attributed to typhoid fever in Kenya (WHO, 2023). Hence, we estimate the disease induced death rate  $\delta_1 = 4 \text{ } 100 = 0.04$ . We calculate the recruitment rate into the susceptible class using the expression for the state of the model at the disease-free equilibrium point,  $S_0 = \frac{\lambda}{\mu}$ , which yields,  $\lambda = \mu S_0 = 0.01493 \times 130000 = 1941$ . All parameters used in model analysis and numerical simulation are given in **Table 3**.

### 6.1.1 Numerical Results

Numerical simulations were conducted to explore the evolution of the transmission dynamics of typhoid fever disease taking into account the direct and indirect modes of transmission alongside the efficacy of control measures such as vaccination and the psychological factor of fear. Using the parameter values given in **Table 3** we simulated the model system for equations (1)-(5) with initial states given as  $S = 130,000$ ,  $I_h = 1265$ ,  $I_e = 9442$ ,  $R = 5000$ , and the initial state for the bacteria population  $B = 145707$ . The parameters for the psychological factor of fear  $\psi_f$ , vaccination  $\alpha$ , and discharge rates  $(\eta_1, \eta_2)$  were varied from a baseline value of 0 to a maximum value of 1, in order to determine their impact on the transmission dynamics. **Figure 4** and **Figure 5** shows the modelling outcomes when psychological factor of fear  $\psi_f$  and

vaccination are either varied, ranging from a low rate of 0 to a high efficacy rate of 1, high efficacy rate of 1, or fixed at a low baseline rate of 0.1 and a high rate of 0.9 respectively. Meanwhile, key parameters are varied to observe their effects on the modelling outcomes

**Table 3: Parameter Values**

Parameter	Value	Unit	Source
$\lambda$	1941	$month^{-1}$	Calculated
$\mu$	0.01493	$month^{-1}$	Calculated
$\psi_f$	Varied (0-1)	-	
$\omega$	0.33	$month^{-1}$	(Edward, 2017)
$\varepsilon_1$	0.0625	$month^{-1}$	(Chamuchi et al., 2014)
$\varepsilon_2$	0.0625	$month^{-1}$	(Chamuchi et al., 2014)
$\eta_1$	Varied (0-1)	-	
$\eta_2$	Varied (0-1)	-	
$\alpha$	Varied (0-1)	-	
$\delta_1$	0.0400	$month^{-1}$	Calculated
$\delta_2$	0.0503	$month^{-1}$	Estimated
$\rho$	0.5	$month^{-1}$	(Edward & Nyerere, 2017)
$\tau$	0.0007	$month^{-1}$	Estimated
$r$	0.00001	$month^{-1}$	Estimated
$K$	500000	$month^{-1}$	(Matsebula, 2021)
$C_h$	0.1533	$month^{-1}$	(Edward, 2017)
$C_e$	0.8133	$month^{-1}$	Estimated

**Figure 2** shows the trend of the typhoid fever model when all the parameter values are constant. As a result of proper sanitation, good personal hygiene, and effective vaccination, the number of susceptible populations gradually declines and the infection

rate is low. The infectious classes  $I_h(t)$  and  $I_e(t)$  exhibits an exponential rise and decreases gradually to a point of stationary equilibrium. The recovered population gradually increases with time up to a specific point before establishing a steady state. We can observe that the bacteria concentration grows gradually over time, reaching a maximum at which the equilibrium point is attained.

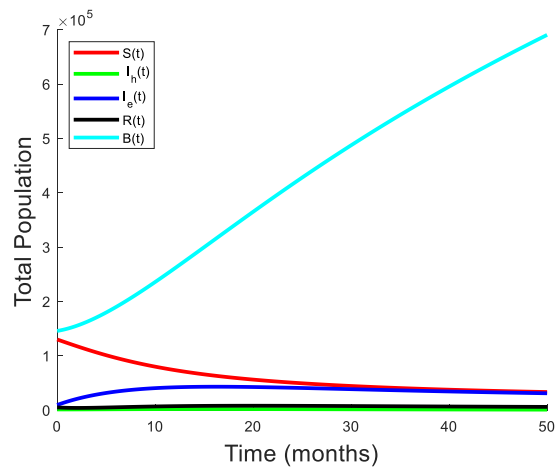


**Figure 2:** Numerical Solution of the Model.

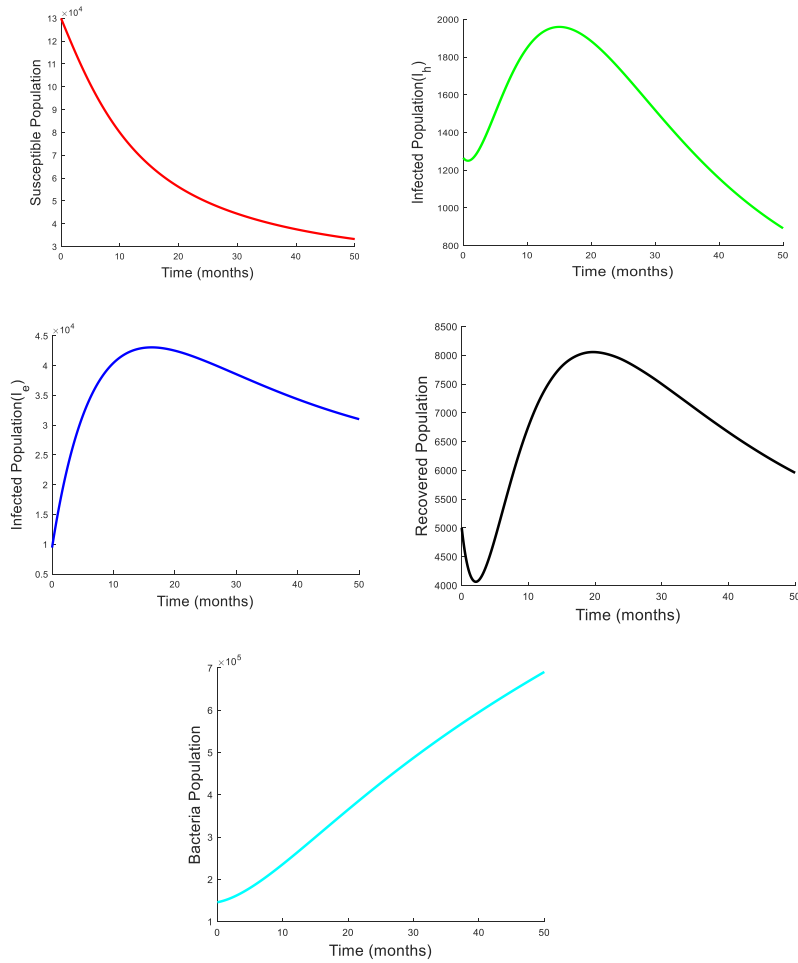


**Figure 3:** Subplots of the Model

**Figure 4–Figure 5** show the effects of varying  $\psi_f$ , on both human and bacteria populations when  $\alpha$  is fixed at low baseline rate of 0.1 and a high efficacy rate of 0.9 respectively. The susceptible population decreases significantly when the psychological factor of fear,  $\psi_f$ , is low, and decreases even further when paired with low vaccination rates (see **Figure 4a–4b**). However, when the psychological factor of fear is high, specifically within the range of 0.9 to 1, even with low vaccination rates, fewer susceptible individuals become infected with typhoid fever. Better results are achieved when both vaccination and the psychological factor of fear are sustained between 0.9 and 1. The number of infected populations is significantly decreased with steady increase in psychological factor of fear,  $\psi_f$ , from 0 to 1 (see **Figure 4c–4f**). Similarly, recovered populations,  $R$ , are further reduced with an increase in  $\psi_f$  (see **Figure 5a–5b**). **Figure 5c–5d**, show that, the bacteria concentration is reduced by high rates of  $\psi_f$ . Better results are achieved when psychological factor of fear,  $\psi_f$  and

vaccination rates,  $\alpha$  are both steadily increased to high efficacy rates. The results imply that, when both fear and vaccination rates are high, the spread of typhoid fever is effectively controlled.

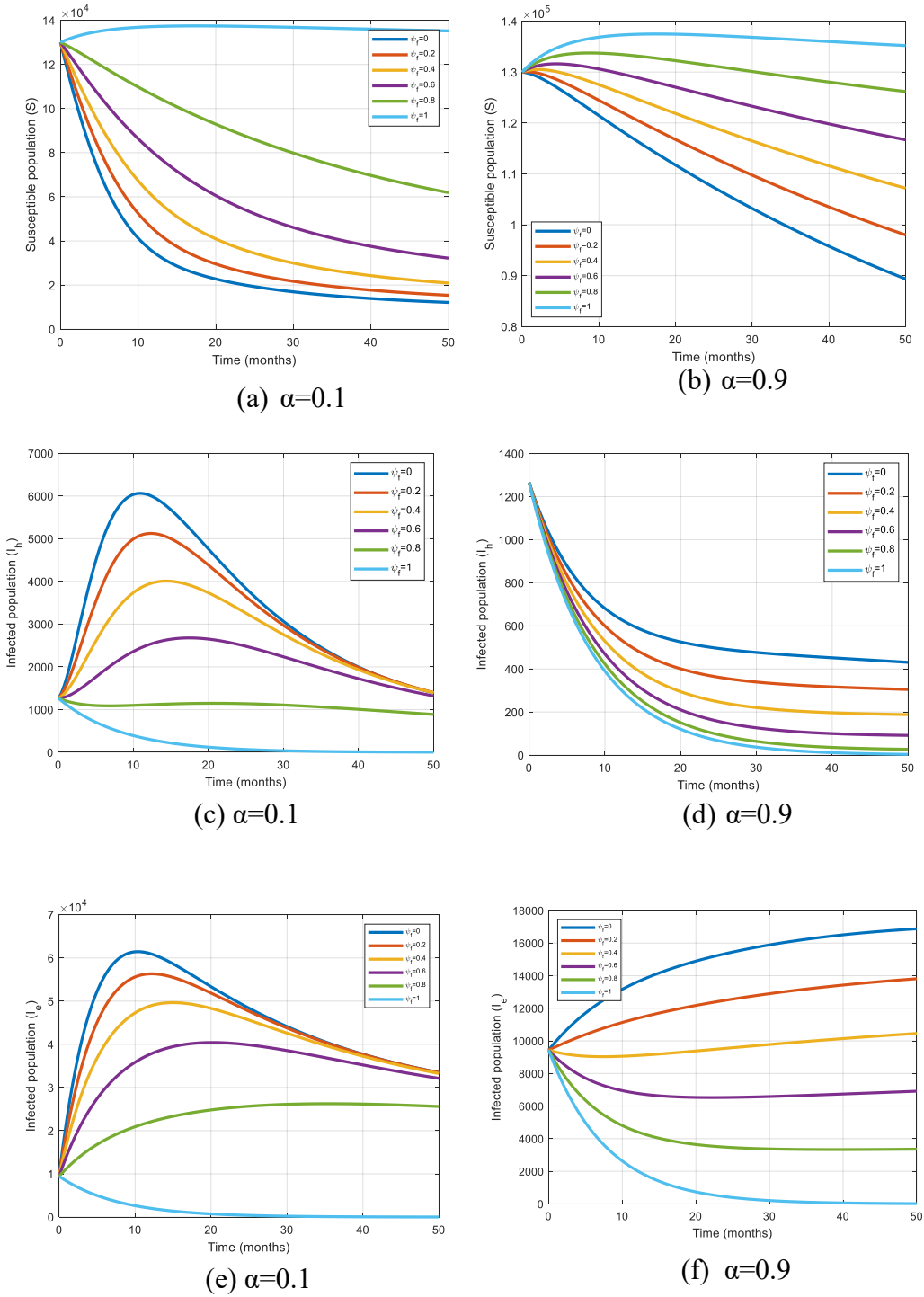
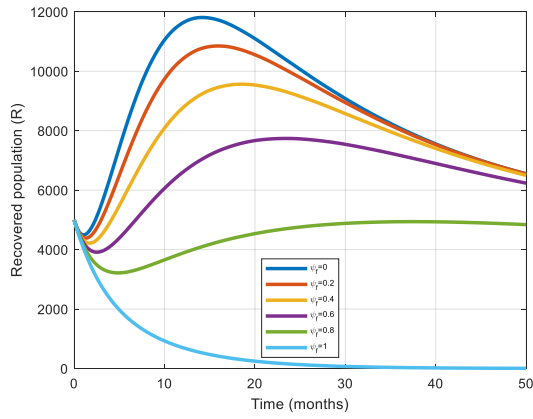
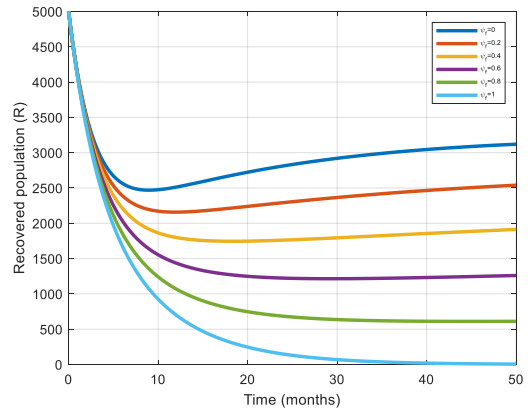


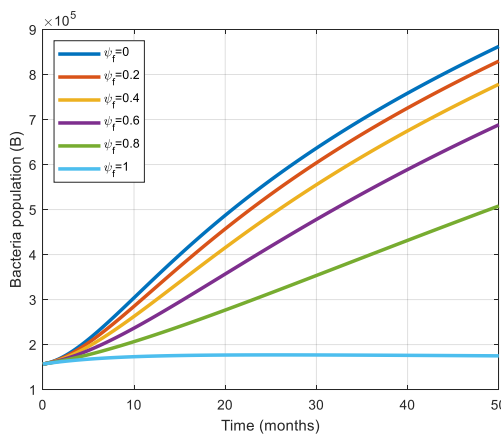
**Figure 4:** Effects of varying  $\psi_f$  on human populations when  $\alpha$  is fixed at 0.1 and 0.9 respectively.



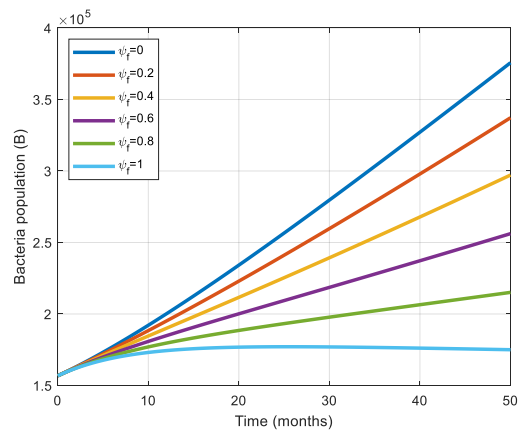
(a)  $\alpha=0.1$



(b)  $\alpha=0.9$



(c)  $\alpha=0.1$



(d)  $\alpha=0.9$

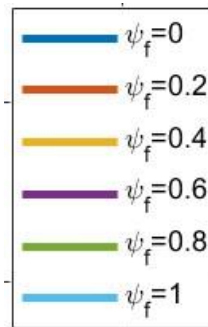


**Figure 5:** Effects of varying  $\psi_f$  on recovered and bacteria populations when  $\alpha$  is fixed at 0.1 and 0.9 respectively.

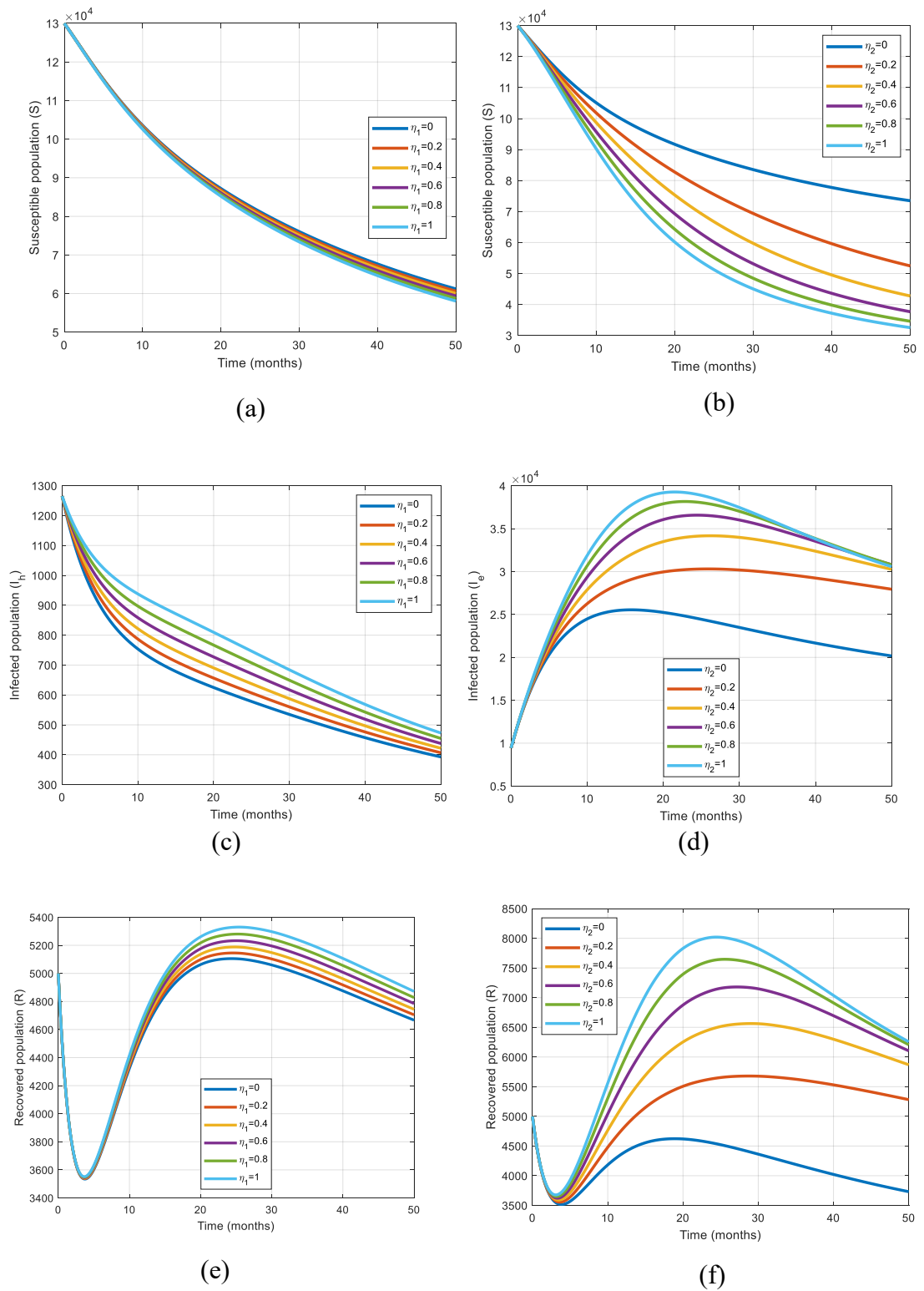


**Figure 6:** Effects of Varying  $\eta_1$  and  $\eta_2$  when  $\alpha = 0.5$  and  $\psi_f = 0.5$ .

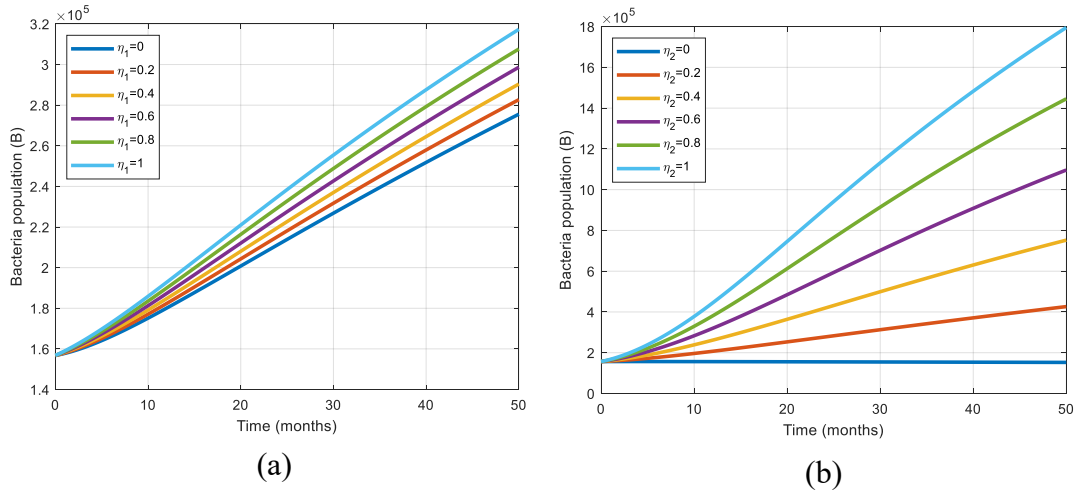


**Figure 7:** Effects of Varying  $\eta_1$  and  $\eta_2$  when  $\alpha = 0.5$  and  $\psi_f = 0.5$ .

**Figure 6-Figure 7** show the effects of varying  $\eta_1$  and  $\eta_2$ , on both human and bacteria populations when  $\alpha$  and  $\psi_f$  are fixed at rate of 0.5. The susceptible population decreases significantly when the discharge rates  $\eta_1$  and  $\eta_2$  are high (see **Figure 6a-6b**) even when paired with the psychological factor of fear and vaccination,  $\psi_f$  and  $\alpha$ , fixed at 0.5. The number of infected populations is significantly increased with steady increase in  $\eta_1$  and  $\eta_2$  from 0 to 1 (see **Figure 6c-6d**). Similarly, recovered populations,  $R$ , are increased with an increase in  $\eta_1$  and  $\eta_2$  (see **Figure 6e-6f**). **Figure 7a-7b**, show that, the bacteria concentration is reduced by low rates of  $\eta_1$  and  $\eta_2$ . Great results are achieved when the discharge rates, of  $\eta_1$  and  $\eta_2$  are both steadily decreased to low rates. The results conclude that, managing discharge rates is important for better overall disease control.

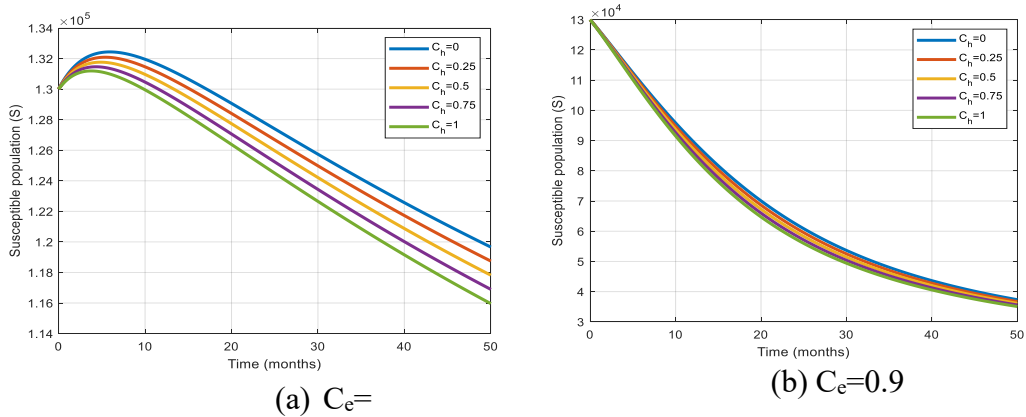
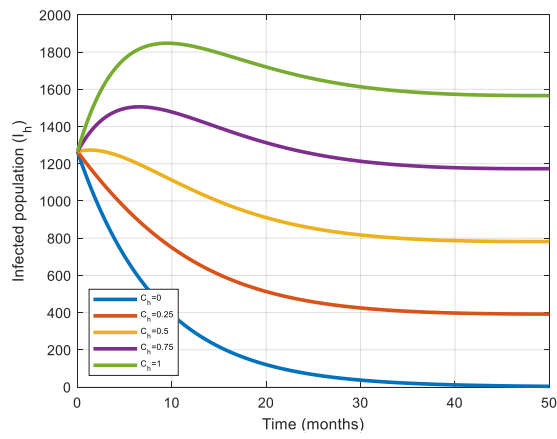
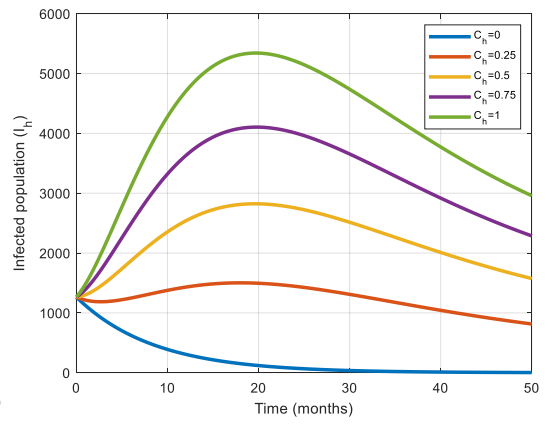


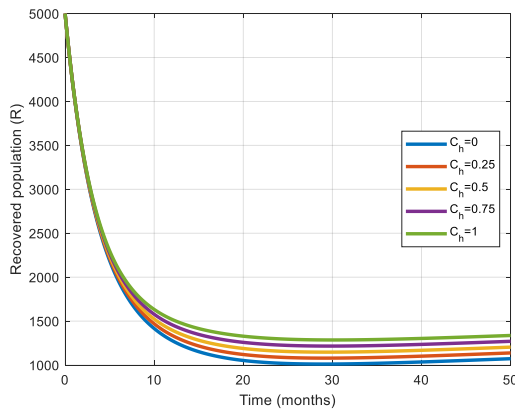
**Figure 8:** Effects of Varying  $C_h$  on the susceptible population when  $C_e$  is fixed at 0.1 and 0.9 respectively.



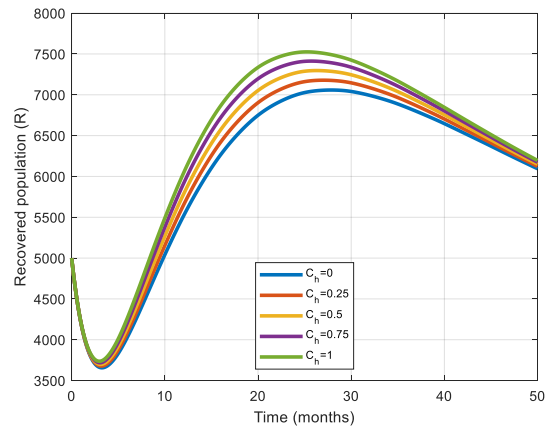
(a)  $C_e=0.1$



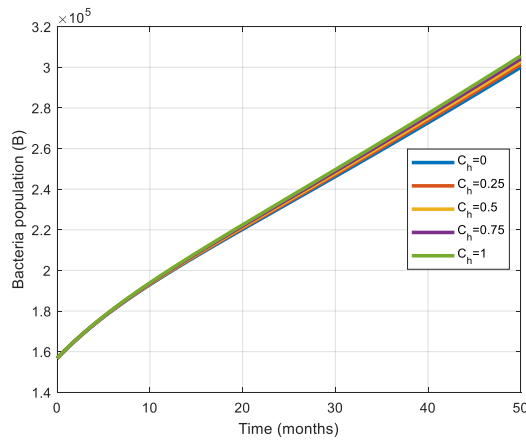
(b)  $C_e=0.9$



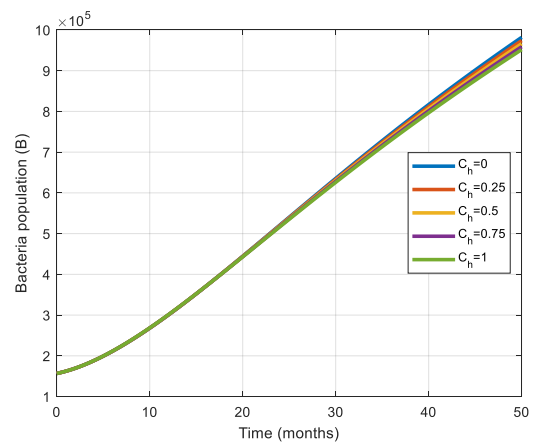
(c)  $C_e=0.1$



(d)  $C_e=0.9$



(e)  $C_e=0.1$



(f)  $C_e=0.9$

**Figure 9:** Effects of Varying  $C_h$  when  $C_e$  is fixed at 0.1 and 0.9 respectively.

**Figure 8-Figure 9** show the effects of varying  $C_h$ , on both human and bacteria populations when  $C_e$  is fixed at low baseline rate of 0.1 and a high efficacy rate of 0.9 respectively. The susceptible population decreases significantly when the direct contact rate,  $C_h$ , is high, and decreases even further when paired with low indirect contact rate. However, when the  $C_e$  is high, specifically within the range of 0.9 to 1, even with low direct rates, more susceptible individuals become infected with typhoid fever (see **Figure 8a-8b**). Better results are achieved when both indirect contact rate and direct contact rate are sustained at low rates of 0.1. The number of infected populations is significantly increased with steady increase in direct contact rate,  $C_h$ , from 0 to 1 (see **Figure 9a-9b**). The recovered populations,  $R$ , is increased with an increase in  $C_h$  (see **Figure 9c-6d**). **Figure 9e-9f**, show that, the bacteria concentration is increased by high rates of  $C_h$ . Desirable results are achieved when direct contact rate,  $C_h$  and indirect contact rates,  $C_e$  are both reduced.

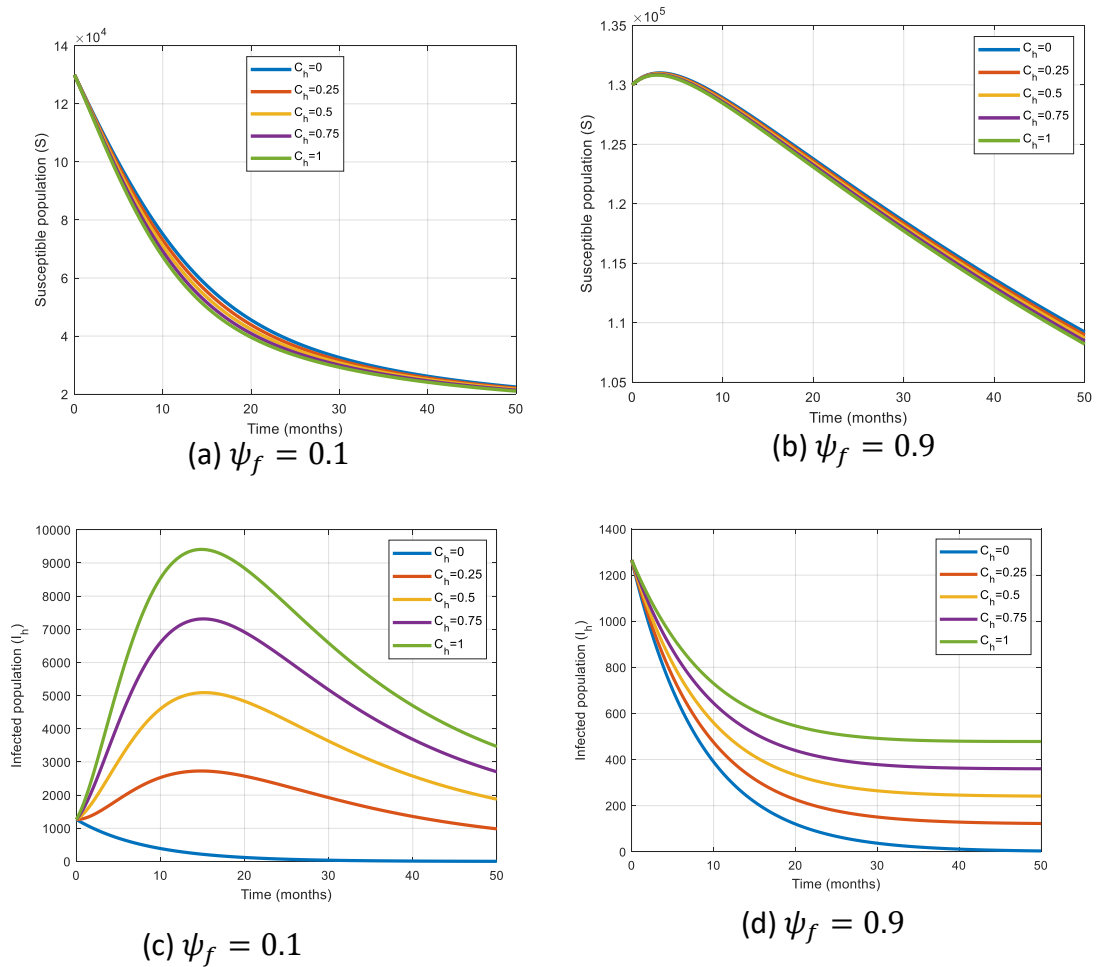
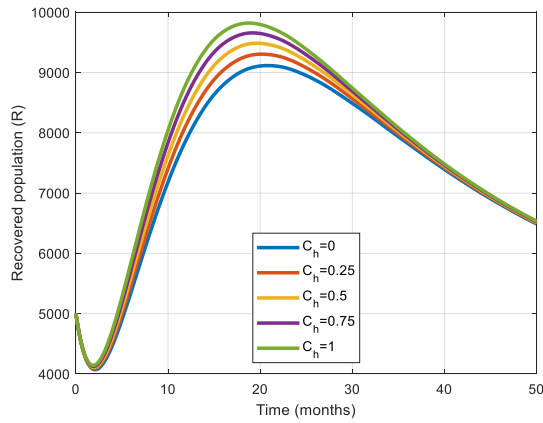
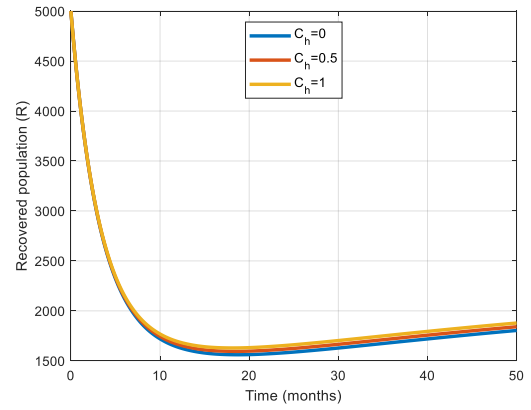


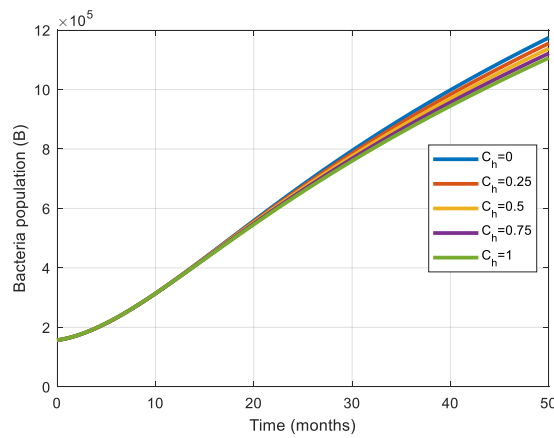
**Figure 10:** Effects of Varying  $C_h$  when  $\psi_f$  is fixed at 0.1 and 0.9 respectively.



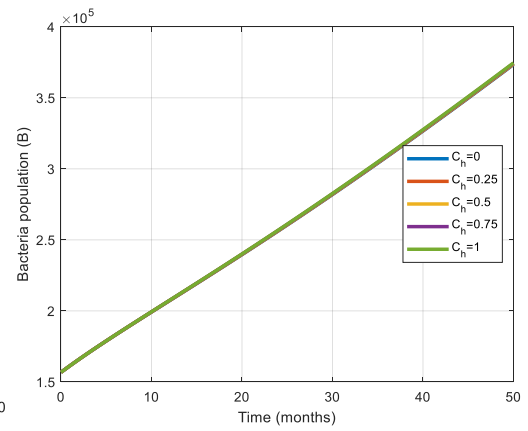
(a)  $\psi_f = 0.1$



(b)  $\psi_f = 0.9$



(c)  $\psi_f = 0.1$



(d)  $\psi_f = 0.9$

**Figure 11:** Effects of Varying  $C_h$  when  $\psi_f$  is fixed at 0.1 and 0.9 respectively

**Figure 10-Figure 11** show the effects of varying  $C_h$ , on both human and bacteria populations when  $\psi_f$  is fixed at low baseline rate of 0.1 and a high efficacy rate of 0.9 respectively. The susceptible population decreases significantly when  $C_h$ , is high, and decreases even further when paired with low psychological factor of fear rates. However, when the psychological factor of fear is high, specifically within the range of 0.9 to 1, even with low direct contact rates, fewer susceptible individuals become infected with typhoid fever disease (see **Figure 10a–10b**). Preferable results are achieved when direct contact rate is sustained at low rates and the psychological factor of fear are sustained between 0.9 and 1. The number of infected populations is significantly increased with decrease in psychological factor of fear and high direct contact rates within the range of 0 to 1. However, the infected population is reduced by high rates of the psychological factor of fear and low direct contact rates (see

Figure 10c–10d). Similarly, recovered populations,  $R$ , are reduced with an increase in  $\psi_f$  (see Figure 11a–11b). Figure 11c-11b, show that, the bacteria concentration is reduced by high rates of  $\psi_f$  and low rates of  $C_h$ .

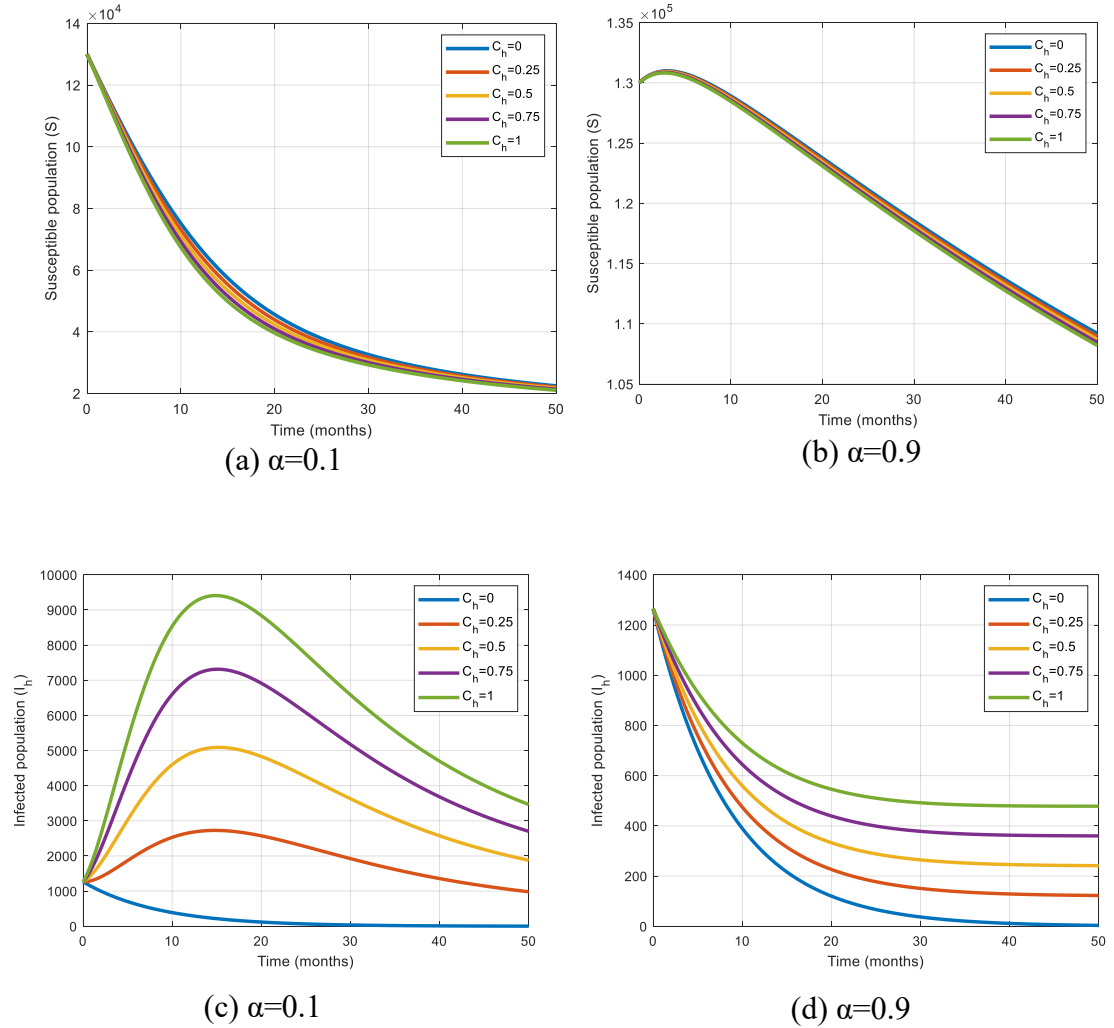
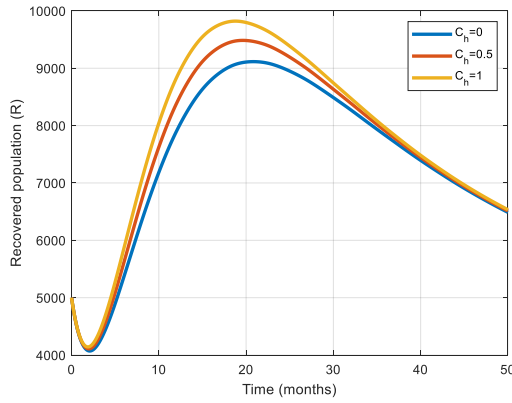
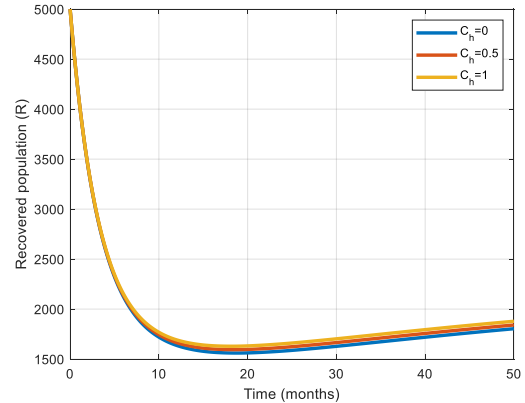


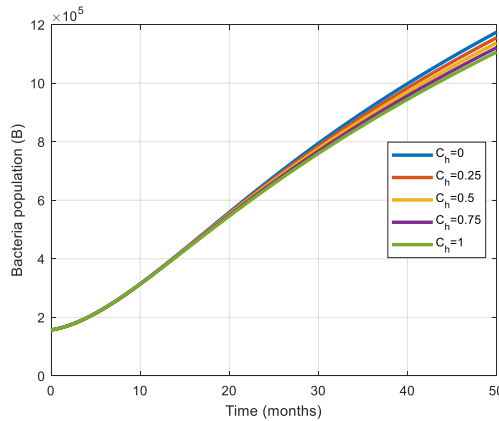
Figure 12: Effects of Varying  $C_h$  when  $\alpha$  is fixed at 0.1 and 0.9 respectively.



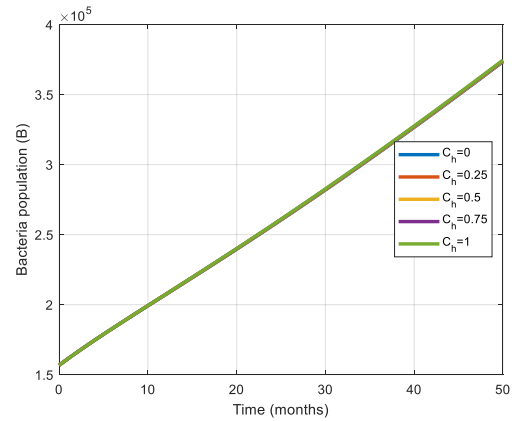
(a)  $\alpha=0.1$



(b)  $\alpha=0.9$



(c)  $\alpha=0.1$



(d)  $\alpha=0.9$

**Figure 13:** Effects of Varying  $C_h$  when  $\alpha$  is fixed at 0.1 and 0.9 respectively

**Figure 12–Figure 13** show the effects of varying  $C_h$ , on both human and bacteria populations when  $\alpha$  is fixed at low baseline rate of 0.1 and a high efficacy rate of 0.9 respectively. The susceptible population reduces significantly when the direct contact rate  $C_h$ , is high, and decreases even further when coupled with low vaccination rates (see **Figure 12a–12b**). However, when the vaccination aspect is high, specifically within the range of 0.9 to 1, even with low direct contact rates, fewer susceptible individuals become infected with typhoid fever. Better results are attained when vaccination is sustained between 0.9 and 1 and the direct contact rates are low. The number of infected populations is significantly increased with steady increase in direct contact rates,  $C_h$ , from 0 to 1 (see **Figure 12c–12d**). Similarly, recovered populations,  $R$ , are further reduced with a decrease in  $C_h$  (see **Figure 13a–13b**). **Figure 13c–13d**, show that, the bacteria concentration is reduced by low rates of  $C_h$ . More Suitable

results are achieved when direct contact rates,  $C_h$  are reduced and vaccination rates,  $\alpha$  are steadily increased to high efficacy rates.

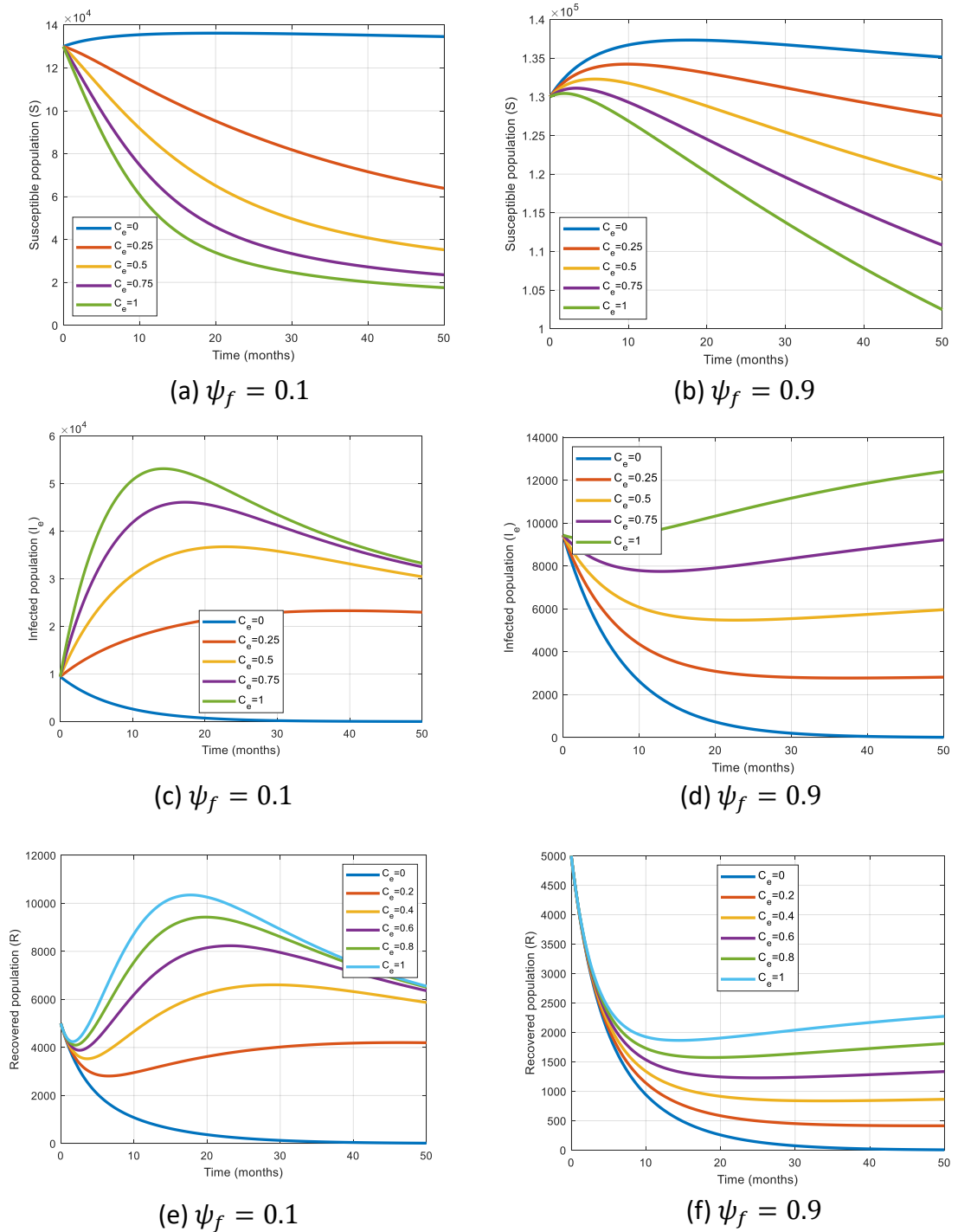
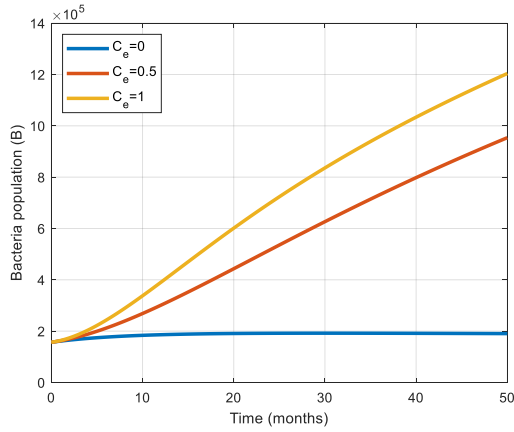
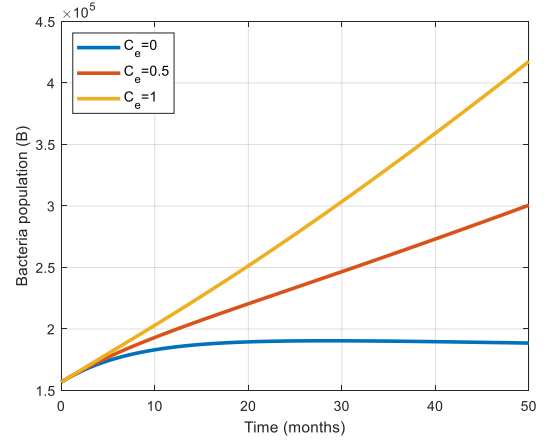


**Figure 14:** Effects of Varying  $C_e$  when  $\psi_f$  is fixed at 0.1 and 0.9 respectively.



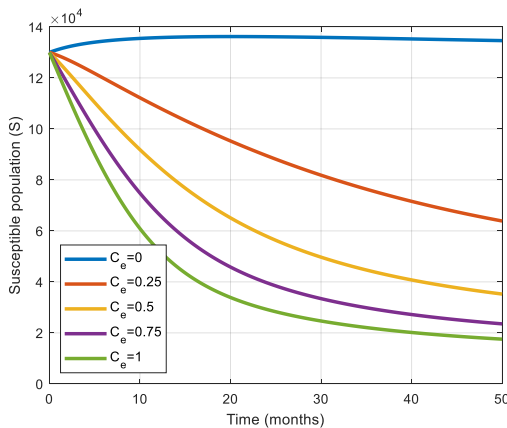
(a)  $\psi_f = 0.1$



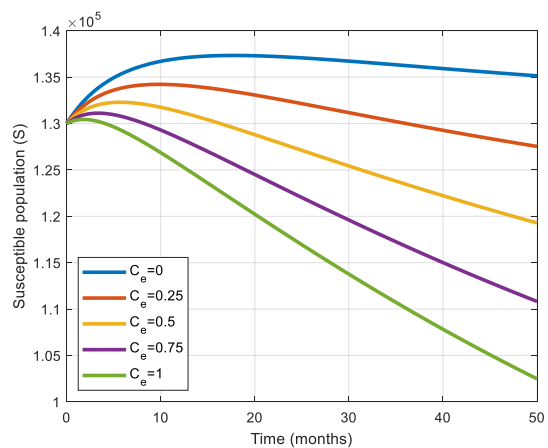
(b)  $\psi_f = 0.1$

**Figure 15:** Effects of Varying  $C_e$  when  $\psi_f$  is fixed at 0.1 and 0.9 respectively.

**Figure 14–Figure 15** show the effects of varying  $C_e$ , on both human and bacteria populations when  $\psi_f$  is fixed at low baseline rate of 0.1 and a high efficacy rate of 0.9 respectively. The susceptible population reduces significantly with increased indirect contact rates and decreased further when paired with low psychological factor of fear  $\psi_f$  (see **Figure 14a–14b**). The infected population is increased by high indirect contact rates and significantly reduced by high rates of psychological factor of fear (see **Figure 14c–14d**). **Figure 14e–14f** show that, the recovered population significantly increases with increase in indirect contact rate. **Figure 15a–15b** reveal that the bacteria concentration is reduced by low rates of indirect contact rates and high rates of psychological factor of fear.



(a)  $\alpha=0.1$



(b)  $\alpha=0.9$

**Figure 16:** Effects of Varying  $C_e$  when  $\alpha$  is fixed at 0.1 and 0.9 respectively.

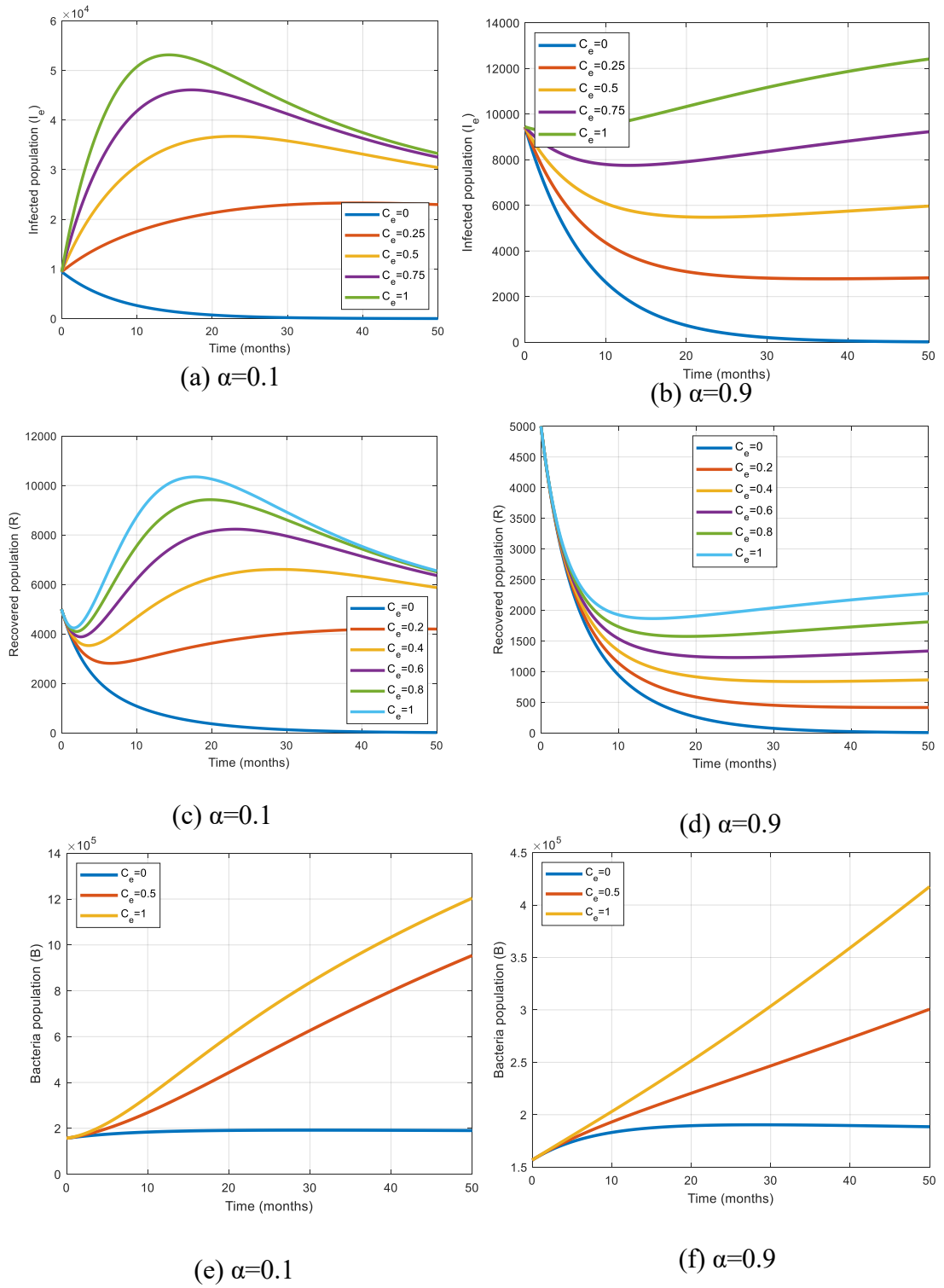


**Figure 17:** Effects of Varying  $C_e$  when  $\alpha$  is fixed at 0.1 and 0.9 respectively.

**Figure 16–Figure 17** show the effects of varying  $C_e$ , on both human and bacteria populations when  $\alpha$  is fixed at low baseline rate of 0.1 and a high efficacy rate of 0.9 respectively. The susceptible population increases significantly when the indirect contact rate  $C_e$  is high, and increases when paired with low vaccination rates (see **Figure 16a–16b**). However, when the vaccination aspect is high, specifically within the range of 0.9 to 1, even with low indirect rates, fewer susceptible individuals become infected with typhoid fever. Better results are attained when vaccination is sustained between 0.9 and 1 and the indirect contact rate are low. The number of infected populations is significantly increased with steady increase in indirect contact rate,  $C_e$ , from 0 to 1 (see **Figure 17a–17d**). Similarly, recovered populations,  $R$ , are further reduced with a decrease in  $C_e$  (see **Figure 17e–17f**). **Figure 17g–17h**, show that, the bacteria concentration is reduced by low rates of  $C_e$ . Valuable outcomes are achieved when direct contact rates,  $C_e$  are reduced and vaccination rates,  $\alpha$  is steadily increased to high efficacy rates.

## CHAPTER FIVE

### DISCUSSION, CONCLUSION AND RECOMMENDATIONS

#### 5.1 DISCUSSION AND CONCLUSION

We presented a deterministic model to examine the interplay between human responses driven by the psychological factor of fear of infection and vaccination efforts in the overall transmission dynamics of typhoid fever, while taking into consideration both the direct and indirect modes of transmission. Applying standard mathematical techniques, we studied the qualitative behavior of the deterministic model where established the feasibility region for the typhoid fever model system, calculated both the disease-free and endemic equilibrium points and determined the necessary conditions for their local and global stability. The typhoid fever model reproduction number  $R_0$  was established using the next generation matrix method and distinct pathways for the transmission of infection were identified, shedding light on the crucial interactions among key population groups fueling the spread of the disease.

Model results show that, heightened psychological factor of fear of typhoid fever disease correspond with a decrease in infection rates. Elevated levels of  $\psi_f$  indicate greater selfresponsiveness to the disease and fewer infected individuals, thus reducing the pool of potential carriers. This in turn prompts individuals to avoid contaminated water sources, uphold personal hygiene, and ensure proper sanitation, in turn lowering bacterial concentrations in the environment. Further, the model results showed that elevated incidences of typhoid fever correlate with declining immunity post treatment with recovered individuals becoming susceptible to infection, vaccine hesitancy, waning vaccine efficacy on vaccinated populations and reduced psychological factor of fear resulting in less caution when interacting with possible contaminated individuals or environment. Numerical simulations further revealed that indirect mode of transmission was exacerbated by high bacteria concentration in the environment which is replenished by discharge rates from the infected populations. The combined elevated discharge rates increase the infection rate and low sustained discharge rates reduces the transmission rate as shown in **Figure 6** and **Figure 7**.

The shedding of the bacteria from the infected classes had a much impact on the bacteria population in the environment. The growth of this bacteria was associated

with the significant contribution of Salmonella Typhi from the infected humans. From these observations, we deduced that, environmental transmission is associated with the increased discharge rates which replenish the bacteria concentration. Additionally, avoiding contact with contaminated food and water reduces typhoid fever infection significantly through direct and indirect mode of transmission. Furthermore, when the psychological factor of fear and vaccination rates are sustained at high levels, the contact rate is reduced as shown in **Figure 6-Figure 17**.

Typhoid fever although contained in some parts of Kenya, continues to cause morbidity and mortality particularly to vulnerable informal settlements with low resilience to proper sanitation and safe drinking water with infants and school-aged children most affected. This has resulted in several typhoid fever outbreaks over the recent years. The Kenyan constitution recognizes drinking treated water as a basic human right. From 2010, resource allocation was increased to support water and sanitation access to clean water in the urban informal settlements within Nairobi (Ng et al., 2023). In addition, the Government of Kenya made efforts to expand treated water sources, upgrade the piping systems and introduce an aerial water distribution source in a bid to tackle sanitation and reduce transmission of infectious diseases like typhoid fever and cholera (Ng et al., 2023).

Despite these noble efforts, adequate mitigation efforts to contain typhoid fever in endemic regions continue to face significant hurdles due to poverty, population displacements, inadequate health infrastructure, cultural and religious beliefs, community norms, vaccine hesitancy, insufficient funding to sustain vaccination efforts and adequate infrastructure to support proper sanitation due to government priorities among others. Our model results suggest that increased vaccination efforts particularly safeguard vulnerable populations like infants and school-aged children, owing to the fact they may lack the psychologically capacity to protect themselves from contaminated sources. Numerical simulations further revealed that combined effects of increased vaccination and heightened psychological factor of fear of typhoid fever play a vital role in preventing typhoid fever transmission, resulting in less bacterial shedding into the environment, as shown in **Figure 4-Figure 5**. In the absence of widespread vaccination against typhoid fever, an increase in the psychological factor of fear of typhoid fever disease is still quite effective in

significantly reducing disease transmission in the appropriate demography as shown in this study. The proposed strategies suggested in this study could further support typhoid fever mitigation strategies even in regions with limited resources as self-responsiveness achieves equally good results in containing the disease, even in the absence of vaccination. The proposed model results will further accelerate the achievement of 2030 Sustainable Development Goal (SDG) aimed at improving health and well-being.

## **5.2 RECOMMEDATIONS**

Further research could consider the inclusion of demographic aspects such as age and gender, spatial aspects, pathogen detection, pathogen characterization, epidemiological surveillance among others, in the typhoid fever mathematical models.

By broadening the scope of these models, researchers will be better equipped to simulate realistic scenarios, guiding policy makers and healthcare professionals in preventing and controlling typhoid fever outbreaks.

## REFERENCES

- Addy, A. (2024). Vaccine Production and Distribution Challenges: An AI-Assisted Technologies for the Overcoming of Logistical Hurdles Faced by Sub-Saharan Africa with focus on Ghana. *Journal of Health, Medicine and Nursing, February*. <https://doi.org/10.7176/jhmn/113-04>
- Adi, D. (2018). *Investigation of a typhoid fever epidemic in Moyale Sub-County, Kenya, 2014–2015*. 1–5.
- Antillón, M., Warren, J. L., Crawford, F. W., Weinberger, D. M., Kürüm, E., Pak, G. D., Marks, F., & Pitzer, V. E. (2017). The burden of typhoid fever in low- and middle-income countries: A meta-regression approach. *PLoS Neglected Tropical Diseases, 11*(2), 1–21. <https://doi.org/10.1371/journal.pntd.0005376>
- Ayoola, T. A. (2021). Modelling and optimal control analysis of typhoid fever. *Journal of Mathematical and Computational Science, 11*(6), 6666–6682. <https://doi.org/10.28919/jmcs/6262>
- Castillo-chavez, C. (2001). *R0 stability*. February.
- Chamuchi, M. N., Sigey, J. K., Okello, J. a, & Okwoyo, J. M. (2014). *SII C R Model and Simulation of the*. 2(3), 109–116.
- Duncan Steele, A., Carey, M. E., Kumar, S., MacLennan, C. A., Ma, L. F., Diaz, Z., & Zaidi, A. K. M. (2020). Typhoid conjugate vaccines and enteric fever control: Where to next? *Clinical Infectious Diseases, 71*(Suppl 2), S185–S190. <https://doi.org/10.1093/cid/ciaa343>
- Edward, S. (2017). A Deterministic Mathematical Model for Direct and Indirect Transmission Dynamics of Typhoid Fever. *OALib, 04*(05), 1–16. <https://doi.org/10.4236/oalib.1103493>
- Edward, S., & Nyerere, N. (2017). *Modelling Typhoid Fever with Education , Vaccination and Treatment*. 1(1), 44–52. <https://doi.org/10.11648/j.engmath.20160101.14>
- Gauld, J. S., Hu, H., Klein, D. J., & Levine, M. M. (2018). Typhoid fever in Santiago, Chile: Insights from a mathematical model utilizing venerable archived data from a successful disease control program. *PLoS Neglected Tropical Diseases, 12*(9), 1–18. <https://doi.org/10.1371/journal.pntd.0006759>
- James, O., Olanrewaju, M., Olaronke, H., Abiodun, F., Oshinubi, K., Adinoyi, A., Abosedo, T., & Oluwasegun, J. (2021). Results in Physics Direct and indirect transmission of typhoid fever model with optimal control. *Results in Physics, 27*, 104463. <https://doi.org/10.1016/j.rinp.2021.104463>
- Kailan Suhuyini, A., & Seidu, B. (2023). A mathematical model on the transmission dynamics of typhoid fever with treatment and booster vaccination. *Frontiers in Applied Mathematics and Statistics, 9*. <https://doi.org/10.3389/fams.2023.1151270>

- Kaluse, P. S., Bhatt, N., & Bankar, N. (2021). *Study of Typhoid Fever : A Review*. 33, 286–291. <https://doi.org/10.9734/JPRI/2021/v33i39A32172>
- Kanyi, E., Afolabi, A. S., & Onyango, N. O. (2021). *Mathematical Modeling and Analysis of Transmission Dynamics and Control of Schistosomiasis*. 2021.
- Karunditu, J. W., Kimathi, G., & Osman, S. (2019). Mathematical Modeling of Typhoid Fever Disease Incorporating Unprotected Humans in the Spread Dynamics. *Journal of Advances in Mathematics and Computer Science*, 32(3), 1–11. <https://doi.org/10.9734/jamcs/2019/v32i330144>
- Kim, C. L., Cruz Espinoza, L. M., Vannice, K. S., Tadesse, B. T., Owusu-Dabo, E., Rakotozandrindrainy, R., Jani, I. V, Teferi, M., Bassiahi Soura, A., Lunguya, O., Steele, A. D., & Marks, F. (2022). The Burden of Typhoid Fever in Sub-Saharan Africa: A Perspective. *Research and Reports in Tropical Medicine, Volume 13*(February 2022), 1–9. <https://doi.org/10.2147/rrtm.s282461>
- Matsebula, L. (2021). *Mathematical analysis of typhoid fever transmission dynamics with seasonality and fear*. 1–27.
- Meiring, J. E., Giubilini, A., Savulescu, J., Pitzer, V. E., & Pollard, A. J. (2019). Generating the Evidence for Typhoid Vaccine Introduction: Considerations for Global Disease Burden Estimates and Vaccine Testing Through Human Challenge. *Clinical Infectious Diseases : An Official Publication of the Infectious Diseases Society of America*, 69(Suppl5), S402–S407. <https://doi.org/10.1093/cid/ciz630>
- Mina, S. A., Hasan, M. Z., Hossain, A. K. M. Z., Barua, A., Mirjada, M. R., & Chowdhury, A. M. M. A. (2023). The Prevalence of Multi-Drug Resistant Salmonellatyphi Isolated From Blood Sample. *Microbiology Insights*, 16, 117863612211507. <https://doi.org/10.1177/11786361221150760>
- Mushanyu, J., Nyabadza, F., Muchatibaya, G., Mafuta, P., & Nhawu, G. (2018). Assessing the potential impact of limited public health resources on the spread and control of typhoid. *Journal of Mathematical Biology*, April 2019. <https://doi.org/10.1007/s00285-018-1219-9>
- Mushayabasa, S. (2016). Modeling the impact of optimal screening on typhoid dynamics. *International Journal of Dynamics and Control*, 4(3), 330–338. <https://doi.org/10.1007/s40435-014-0123-4>
- Mutua, J. M., Barker, C. T., & Vaidya, N. K. (2017). Modeling Impacts of Socioeconomic Status and Vaccination Programs on Typhoid Fever Epidemics. *Electronic Journal of Differential Equations*, 24, 63–74.
- Ng, E., Lind, M., Audi, A., Ouma, A., Oduor, C., Munywoki, P. K., Agogo, G. O., Odongo, G., Kiplangat, S., Wamola, N., Osita, M. P., Mugoh, R., Ochieng, C., Omballa, V., Mogeni, O. D., Mikoleit, M., Fields, B. S., Montgomery, J. M., Gauld, J., ... Verani, J. R. (2023). *Dynamic Incidence of Typhoid Fever over a 10-Year Period ( 2010 – 2019 ) in Kibera , an Urban Informal Settlement in Nairobi , Kenya*. 1–10. <https://doi.org/10.4269/ajtmh.22-0736>

- Njenga, J. K., & Kipchirchir, I. C. (2024). Modelling Mortality in Kenya. *Asian Research Journal of Mathematics*, 20(1), 1–15. <https://doi.org/10.9734/arjom/2024/v20i1777>
- Nyaberi, H. O., & Musaili, J. S. (2021). Mathematical modeling of the impact of treatment on the dynamics of typhoid. *Journal of the Egyptian Mathematical Society*, 29(1). <https://doi.org/10.1186/s42787-021-00125-8>
- Ryan, K. K. (2021). *Mathematical modelling on the impact of hospitalization in the management of typhoid fever*. University of Eldoret.
- Stanaway, J. D., Atuhebwe, P. L., Luby, S. P., & Crump, J. A. (2020). Assessing the feasibility of typhoid elimination. *Clinical Infectious Diseases*, 71(2), S179–S184. <https://doi.org/10.1093/cid/ciaa585>
- Verelst, F., Willem, L., & Beutels, P. (2016). Behavioural change models for infectious disease transmission: a systematic review (2010–2015). *Journal of The Royal Society Interface*, 13(125). <https://doi.org/10.1098/RSIF.2016.0820>
- Volkova, V. V., Lu, Z., Lanzas, C., Scott, H. M., & Gröhn, Y. T. (2013). Modelling dynamics of plasmid-gene mediated antimicrobial resistance in enteric bacteria using stochastic differential equations. *Scientific Reports*, 3. <https://doi.org/10.1038/srep02463>
- Wesley, C. L., Allen, L. J. S., & Langlais, M. (2010). Models for the spread and persistence of hantavirus infection in rodents with direct and indirect transmission. *Mathematical Biosciences and Engineering*, 7(1), 195–211. <https://doi.org/10.3934/mbe.2010.7.195>
- WHO. (2023). *Weekly bulletin on outbreaks and other emergencies* (Issue April).